

October 22, 2018  
CPT-2003/P.4525

# The anomalous magnetic moment of the muon: a theoretical introduction <sup>1</sup>

Marc Knecht

Centre de Physique Théorique, CNRS-Luminy, Case 907  
F-13288 Marseille Cedex 9, France

---

<sup>1</sup>Based on the lectures delivered at the 41. Internationale Universitätswochen für Theoretische Physik, Schladming, Styria, Austria, February 22 - 28, 2003.

# 1 Introduction

In February 2001, the Muon ( $g-2$ ) Collaboration of the E821 experiment at the Brookhaven AGS released a new value of the anomalous magnetic moment of the muon  $a_\mu$ , measured with an unprecedented accuracy of 1.3 ppm [parts per million]. This announcement has caused quite some excitement in the particle physics community. Indeed, this experimental value was claimed to show a deviation of  $2.6 \sigma$  with one of the most accurate evaluations of the anomalous magnetic moment of the muon within the standard model. It was subsequently shown that a sign error in one of the theoretical contributions was responsible for a sizeable part of this discrepancy, which eventually only amounted to  $1.6 \sigma$ . However, this event had the merit to draw the attention to the fact that low energy but high precision experiments represent real potentialities, complementary to the high energy accelerator programs, for evidencing possible new degrees of freedom, supersymmetry or whatever else, beyond those described by the standard model of electromagnetic, weak, and strong interactions.

Clearly, in order for theory to match such an accurate measurement, calculations in the standard model have to be pushed to their very limits. The difficulty is not only one of having to compute higher orders in perturbation theory, but also to correctly take into account strong interaction contributions involving low-energy scales, where non perturbative effects are important, and which therefore represent a real theoretical challenge. Furthermore, in the meantime the members of experimental team at Brookhaven have further improved upon their measurement. In July 2002, they have announced a new result, in perfect agreement with the one they had obtained about one year and a half before, but with an error lowered down to the 0.7 ppm level. In addition, the theoretical evaluation of a specific and important contribution, called hadronic vacuum polarization, on which we shall have more to say later on, has shown a discrepancy between different data sets that are used as inputs. Depending on the choice between these conflicting data, the discrepancy between the experimental and the theoretical values can be as small as  $1 \sigma$ , certainly not a case for beyond the standard model physics, or can reach the  $3 \sigma$  level, a much more promising situation as far as the possibility of “new physics” is concerned.

The purpose of this account is to give an overview of the main features of the theoretical calculations that have been done in order to obtain accurate predictions for the anomalous magnetic moment of the muon within the standard model. Actually, all three charged leptons,  $e^\pm$ ,  $\mu^\pm$ , and  $\tau^\pm$ , of the standard model can be treated on the same footing, except that the very different values of their masses will induce different sensitivities with respect to the mass scales involved in the higher order quantum corrections. Thus, the anomalous magnetic moment of the electron is almost only [but not quite] sensitive to the electromagnetic interactions of the leptons, and its value is barely affected by strong interaction effects or by weak interaction corrections. On the other hand, the strengths of the latter two types of corrections are enhanced by a considerable factor,  $\sim (m_\tau/m_e)^2 \sim 1.2 \times 10^7$ , in the case of the  $\tau$ , as compared to the electron. The same huge enhancement factor would also affect the contributions coming from degrees of freedom beyond the standard model, so that the measurement of the anomalous magnetic moment of the  $\tau$  would represent the best opportunity to detect new physics. Unfortunately, the very short lifetime of the  $\tau$  lepton which, precisely because of its high mass, can also decay into hadronic states, makes such a measurement impossible at present. The muon lies somewhat in the intermediate range of mass scales <sup>2</sup> and its lifetime still makes a measurement of its anomalous magnetic moment possible. However, in order to obtain an accurate [that is, comparable to the experimental accuracy] prediction, the contributions of all the sectors of the standard model have

---

<sup>2</sup>The corresponding enhancement factor is  $\sim (m_\mu/m_e)^2 \sim 4 \times 10^4$ .

to be known very precisely. Therefore, although the other two lepton flavours will also be discussed, since this does not really require additional work, the emphasis of these lectures will nevertheless be put on the muon.

There exist several excellent reviews and introductions, which the interested reader may consult. As far as the situation up to 1990 is concerned, the collection of articles published in Ref. [1] offers a wealth of information, on both theory and experiment. Very useful accounts of earlier theoretical work are presented in Refs. [2, 3]. Among the more recent reviews, Refs. [4, 5, 6, 7, 8] are most informative. I shall not touch the subject of the study of new physics scenarios which might offer an explanation for a possible deviation between the standard model prediction of the magnetic moment of the muon and its experimental value, should such a deviation be confirmed in the future. For this aspect, I refer the reader to [9] and to the articles quoted therein, or to [10] for a list of the recent papers on the subject.

## 2 General considerations

In the context of relativistic quantum mechanics, the interaction of a pointlike spin one-half particle of charge  $e_\ell$  and mass  $m_\ell$  [ $\ell$  stands hereafter for any of the three charged lepton flavours  $e$ ,  $\mu$  or  $\tau$ ] with an external electromagnetic field  $\mathcal{A}_\mu(x)$  is described by the Dirac equation with the minimal coupling prescription,

$$i\hbar \frac{\partial \psi}{\partial t} = \left[ c\boldsymbol{\alpha} \cdot \left( -i\hbar \boldsymbol{\nabla} - \frac{e_\ell}{c} \mathcal{A} \right) + \beta m_\ell c^2 + e_\ell \mathcal{A}_0 \right] \psi. \quad (2.1)$$

In the non relativistic limit, this reduces to the Pauli equation for the two-component spinor  $\varphi$  describing the large components of the Dirac spinor  $\psi$ ,

$$i\hbar \frac{\partial \varphi}{\partial t} = \left[ \frac{(-i\hbar \boldsymbol{\nabla} - (e_\ell/c) \mathcal{A})^2}{2m_\ell} - \frac{e_\ell \hbar}{2m_\ell c} \boldsymbol{\sigma} \cdot \mathbf{B} + e_\ell \mathcal{A}_0 \right] \varphi. \quad (2.2)$$

As is well known, this equation amounts to associate with the particle's spin a magnetic moment

$$\mathbf{M}_s = g_\ell \left( \frac{e_\ell}{2m_\ell c} \right) \mathbf{S}, \quad \mathbf{S} = \hbar \frac{\boldsymbol{\sigma}}{2}, \quad (2.3)$$

with a gyromagnetic ratio predicted to be  $g_\ell = 2$ .

In the context of quantum field theory, the response to an external electromagnetic field is described by the matrix element of the electromagnetic current  ${}^3\mathcal{J}^\rho$  [spin projections and Dirac indices of the spinors are not written explicitly]

$$\langle \ell^-(p') | \mathcal{J}^\rho(0) | \ell^-(p) \rangle = \bar{u}(p') \Gamma^\rho(p', p) u(p), \quad (2.4)$$

with  $[k_\mu \equiv p'_\mu - p_\mu]$

$$\Gamma^\rho(p', p) = F_1(k^2) \gamma^\rho + \frac{i}{2m_\ell} F_2(k^2) \sigma^{\rho\nu} k_\nu - F_3(k^2) \gamma_5 \sigma^{\rho\nu} k_\nu + F_4(k^2) [k^2 \gamma^\rho - 2m_\ell k^\rho] \gamma_5. \quad (2.5)$$

---

<sup>3</sup>In the standard model,  $\mathcal{J}^\rho$  denotes the total electromagnetic current, with the contributions of all the charged elementary fields in presence, leptons, quarks, electroweak gauge bosons,...

This expression of the matrix element  $\langle \ell^-(p') | \mathcal{J}^\rho(0) | \ell^-(p) \rangle$  is the most general that follows from Lorentz invariance, the Dirac equation for the two spinors,  $(\not{p} - m)u(p) = 0$ ,  $\bar{u}(p')(\not{p}' - m) = 0$ , and the conservation of the electromagnetic current,  $(\partial \cdot \mathcal{J})(x) = 0$ . The two first form factors,  $F_1(k^2)$  and  $F_2(k^2)$ , are known as the Dirac form factor and the Pauli form factor, respectively. Since the electric charge operator  $\mathcal{Q}$  is given, in units of the charge  $e_\ell$ , by

$$\mathcal{Q} = \int d\mathbf{x} \mathcal{J}_0(x^0, \mathbf{x}), \quad (2.6)$$

the form factor  $F_1(k^2)$  is normalized by the condition  $F_1(0) = 1$ . The presence of the form factor  $F_3(k^2)$  requires both parity and time reversal invariance to be broken, whereas  $F_4(k^2)$  can be different from zero provided parity is broken. Both  $F_3(k^2)$  and  $F_4(k^2)$  are therefore absent if only electromagnetic and strong interactions are considered [we leave aside the possibility of having a non vanishing vacuum angle in the strong interaction sector]. On the other hand, in the standard model, the weak interactions violate both parity and time reversal symmetry, so that they actually induce non vanishing expressions for these form factors.

The above form factors are defined for  $k^2 < 0$ , and they are real in this region if the current  $\mathcal{J}_\rho(x)$  is hermitian. Due to general properties of quantum field theory, like causality, analyticity, and crossing symmetry, these form factors can be analytically continued into the whole complex  $k^2$  plane with a cut for  $k^2 > 4m_\ell^2$ . They then become complex functions, obeying the Schwartz reflection property  $F_i(k^2)^* = F_i(k^{2*})$ . For  $k^2 > 4m_\ell^2$ , the form factors  $F_i(k^2 + i\epsilon)$  describe the crossed channel matrix element  $\langle \ell^-(p') \ell^+(p) | \mathcal{J}^\rho(0) | 0 \rangle$ . Furthermore, at  $k^2 = 0$ , they describe the residue of the s-channel photon pole in the S-matrix element for elastic  $\ell^+ \ell^-$  scattering.

At tree level in the standard model, one finds

$$F_1^{\text{tree}}(k^2) = 1, \quad F_i^{\text{tree}}(k^2) = 0, \quad i = 2, 3, 4. \quad (2.7)$$

In order to obtain non zero values for  $F_2(k^2)$ ,  $F_3(k^2)$ , and  $F_4(k^2)$  already at tree level, the interaction of the Dirac field with the photon field  $\mathcal{A}_\mu$  would have to depart from the minimal coupling prescription. For instance, the modification  $[\mathcal{F}_{\mu\nu} = \partial_\mu \mathcal{A}_\nu - \partial_\nu \mathcal{A}_\mu, \mathcal{J}^\rho = \bar{\psi} \gamma^\rho \psi]$

$$\begin{aligned} \int d^4x \mathcal{L}_{\text{int}} &= -\frac{e_\ell}{c} \int d^4x \mathcal{J}^\rho \mathcal{A}_\rho \rightarrow \\ &\rightarrow \int d^4x \widehat{\mathcal{L}}_{\text{int}} = -\frac{e_\ell}{c} \int d^4x \left[ \mathcal{J}^\rho \mathcal{A}_\rho + \frac{\hbar}{4m_\ell} a_\ell \bar{\psi} \sigma_{\mu\nu} \psi \mathcal{F}^{\mu\nu} + \frac{\hbar}{2e_\ell} d_\ell \bar{\psi} i \gamma_5 \sigma_{\mu\nu} \psi \mathcal{F}^{\mu\nu} \right] \\ &= -\frac{e_\ell}{c} \int d^4x \widehat{\mathcal{J}}^\rho \mathcal{A}_\rho, \end{aligned} \quad (2.8)$$

with <sup>4</sup>

$$\widehat{\mathcal{J}}_\rho = \mathcal{J}_\rho - \frac{\hbar}{2m_\ell} a_\ell \partial^\mu (\bar{\psi} \sigma_{\mu\rho} \psi) - \frac{\hbar d_\ell}{e_\ell} \partial^\mu (\bar{\psi} i \gamma_5 \sigma_{\mu\rho} \psi), \quad (2.9)$$

leads to

$$\widehat{F}_1^{\text{tree}}(k^2) = 1, \quad \widehat{F}_2^{\text{tree}}(k^2) = a_\ell, \quad \widehat{F}_3^{\text{tree}}(k^2) = d_\ell/e_\ell, \quad \widehat{F}_4^{\text{tree}}(k^2) = 0. \quad (2.10)$$

---

<sup>4</sup>The current  $\widehat{\mathcal{J}}^\rho$  is still a conserved four-vector, therefore the matrix element  $\langle \ell^-(p') | \widehat{\mathcal{J}}^\rho(0) | \ell^-(p) \rangle$  also takes the form (2.4), (2.5), with appropriate form factors  $\widehat{F}_i(k^2)$ .

The equation satisfied by the Dirac spinor  $\psi$  then reads

$$i\hbar \frac{\partial \psi}{\partial t} = \left[ c\boldsymbol{\alpha} \cdot \left( -i\hbar \boldsymbol{\nabla} - \frac{e_\ell}{c} \boldsymbol{\mathcal{A}} \right) + \beta m_\ell c^2 + e_\ell \mathcal{A}_0 + \frac{e_\ell \hbar}{2m_\ell} a_\ell \beta (i\boldsymbol{\alpha} \cdot \mathbf{E} - \boldsymbol{\Sigma} \cdot \mathbf{B}) - \hbar d_\ell \beta (\boldsymbol{\Sigma} \cdot \mathbf{E} + i\boldsymbol{\alpha} \cdot \mathbf{B}) \right] \psi, \quad (2.11)$$

and the corresponding non relativistic limit becomes <sup>5</sup>

$$i\hbar \frac{\partial \varphi}{\partial t} = \left[ \frac{(-i\hbar \boldsymbol{\nabla} - (e_\ell/c)\boldsymbol{\mathcal{A}})^2}{2m_\ell} - \frac{e_\ell \hbar}{2m_\ell c} (1 + a_\ell) \boldsymbol{\sigma} \cdot \mathbf{B} - \hbar d_\ell \boldsymbol{\sigma} \cdot \mathbf{E} + e_\ell \mathcal{A}_0 + \dots \right] \varphi. \quad (2.12)$$

Thus the coupling constant  $a_\ell$  induces a shift in the gyromagnetic factor,  $g_\ell = 2(1 + a_\ell)$ , while  $d_\ell$  gives rise to an electric dipole moment. The modification (2.8) of the interaction with the photon field introduces two arbitrary constants, and both terms produce a *non renormalizable* interaction. Non constant values of the form factors could be generated at tree level upon introducing [11] additional non renormalizable couplings, involving derivatives of the external field of the type  $\square^n \mathcal{A}_\mu$ , which preserve the gauge invariance of the corresponding field equation satisfied by  $\psi$ . In a similar way, one can also introduce terms which induce a nonzero value for  $F_4$ . In a renormalizable framework, like QED or the standard model, calculable non vanishing values for  $F_2(k^2)$ ,  $F_3(k^2)$ , and  $F_4(k^2)$  are generated by the loop corrections. In particular, the latter will likewise induce an *anomalous magnetic moment*

$$a_\ell = \frac{1}{2}(g_\ell - 2) = F_2(0) \quad (2.13)$$

and an electric dipole moment  $d_\ell = e_\ell F_3(0); F_4(0)$ , which corresponds to an axial radius of the lepton, is also called the *anapole moment* [12, 13, 14], and is sensitive to the gradients of the external fields.

If we consider only the electromagnetic and the strong interactions, the current  $\mathcal{J}^\rho$  is gauge invariant, and the two form factors that remain in that case,  $F_1(k^2)$  and  $F_2(k^2)$ , do not depend on the gauges chosen in order to quantize the photon and the gluon gauge fields. This is no longer the case if the weak interactions are included as well, since  $\mathcal{J}^\rho$  now transforms in a non trivial way under a weak gauge transformation, and the corresponding form factors in general depend on the gauge choices. As we have already mentioned above, the zero momentum transfer values  $F_i(0)$ ,  $i = 1, 2, 3, 4$  describe a physical S-matrix element. To the extent that the perturbative S-matrix of the standard model does not depend on the gauge fixing parameters to any order of the renormalized perturbation expansion, the quantities  $F_i(0)$  should define *bona fide* gauge-fixing independent observables.

The computation of  $\Gamma_\rho(p', p)$  is often a tedious task, especially if higher loop contributions are considered. It is therefore useful to concentrate the efforts on computing the form factor of interest, e.g.  $F_2(k^2)$  in the case of the anomalous magnetic moment. This can be achieved upon projecting out the different form factors [15, 16] using the following general expression <sup>6</sup>

$$F_i(k^2) = \text{tr} [\Lambda_i^\rho(p', p)(\not{p}' + m_\ell)\Gamma_\rho(p', p)(\not{p} + m_\ell)] , \quad (2.14)$$

<sup>5</sup>Terms involving the gradients of the external fields  $\mathbf{E}$  and  $\mathbf{B}$  or terms nonlinear in these fields are not shown.

<sup>6</sup>From now on, I most of the time use the system of units where  $\hbar = 1$ ,  $c = 1$ . Other projectors on  $F_2(k^2)$  have also been devised, see e.g. [17], but are not currently used.

with

$$\begin{aligned}
\Lambda_1^\rho(p', p) &= \frac{1}{4} \frac{1}{k^2 - 4m_\ell^2} \gamma^\rho + \frac{3m_\ell}{2} \frac{1}{(k^2 - 4m_\ell^2)^2} (p' + p)^\rho \\
\Lambda_2^\rho(p', p) &= -\frac{m_\ell^2}{k^2} \frac{1}{k^2 - 4m_\ell^2} \gamma^\rho - \frac{m_\ell}{k^2} \frac{k^2 + 2m_\ell^2}{(k^2 - 4m_\ell^2)^2} (p' + p)^\rho \\
\Lambda_3^\rho(p', p) &= -\frac{i}{2k^2} \frac{1}{k^2 - 4m_\ell^2} \gamma_5 (p' + p)^\rho \\
\Lambda_4^\rho(p', p) &= -\frac{1}{4k^2} \frac{1}{k^2 - 4m_\ell^2} \gamma_5 \gamma^\rho.
\end{aligned} \tag{2.15}$$

For  $k \rightarrow 0$ , one has

$$\Lambda_2^\rho(p', p) = \frac{1}{4k^2} \left[ \gamma^\rho - \frac{1}{m_\ell} \left( 1 + \frac{k^2}{m_\ell^2} \right) (p + \frac{1}{2}k)^\rho + \dots \right], \tag{2.16}$$

and

$$(\not{p} + m_\ell) \Lambda_2^\rho(p', p) (\not{p}' + m_\ell) = \frac{1}{4} (\not{p} + m_\ell) \left[ -\frac{k^\rho}{k^2} + \left( \gamma^\rho - \frac{p^\rho}{m_\ell} \right) \frac{k}{k^2} + \dots \right]. \tag{2.17}$$

The last expression behaves as  $\sim 1/k$  as the external photon four momentum  $k_\mu$  vanishes, so that one may worry about the finiteness of  $F_2(0)$  obtained upon using Eq. (2.14). This problem is solved by the fact that  $\Gamma^\rho(p', p)$  satisfies the Ward identity

$$(p' - p)_\rho \Gamma^\rho(p', p) = 0, \tag{2.18}$$

following from the conservation of the electromagnetic current. Therefore, the identity

$$\Gamma^\rho(p', p) = -k_\sigma \frac{\partial}{\partial k_\rho} \Gamma^\sigma(p', p) \tag{2.19}$$

provides the additional power of  $k$  which ensures a finite result as  $k_\mu \rightarrow 0$ .

The presence of three different interactions in the standard model naturally leads one to consider the following decomposition of the anomalous magnetic moment  $a_\ell$ :

$$a_\ell = a_\ell^{\text{QED}} + a_\ell^{\text{had}} + a_\ell^{\text{weak}}. \tag{2.20}$$

The first term,  $a_\ell^{\text{QED}}$ , denotes all the contributions which arise from loops involving only virtual photons and leptons. Among these, it is useful to distinguish those which involve only the same lepton flavour  $\ell$  for which we wish to compute the anomalous magnetic moment, and those which involve loops with leptons of different flavours, denoted collectively as  $\ell'$  [ $\alpha \equiv e^2/4\pi$ ],

$$a_\ell^{\text{QED}} = \sum_{n \geq 1} A_n \left( \frac{\alpha}{\pi} \right)^n + \sum_{n \geq 2} B_n(\ell, \ell') \left( \frac{\alpha}{\pi} \right)^n. \tag{2.21}$$

The second type of contribution,  $a_\ell^{\text{had}}$ , involves also quark loops. Their contribution is far from being limited to the short distance scales, and  $a_\ell^{\text{had}}$  is an intrinsically non perturbative quantity. From a theoretical point of view, this represents a serious difficulty. Finally, at some level of precision, the weak interactions can no longer be ignored, and contributions of virtual Higgs or massive gauge boson

degrees of freedom induce the third component  $a_\ell^{\text{weak}}$ . Of course, starting from the two loop level, a hadronic contribution to  $a_\ell^{\text{weak}}$  will also be present. The remainder of this presentation is devoted to a detailed discussion of these various contributions.

Before starting this guided tour of the anomalous magnetic moments of the massive charged leptons of the standard model, it is useful to keep in mind a few simple considerations:

- The anomalous magnetic moment is a dimensionless quantity. Therefore, the coefficients  $A_n$  above are *universal*, i.e. they do not depend on the flavour of the lepton whose anomalous magnetic moment we wish to evaluate.
- The contributions to  $a_\ell$  of degrees of freedom corresponding to a typical scale  $M \gg m_\ell$  decouple [18], i.e. they are *suppressed* by powers of  $m_\ell/M$ .<sup>7</sup>
- The contributions to  $a_\ell$  originating from light degrees of freedom, characterized by a typical scale  $m \ll m_\ell$  are *enhanced* by powers of  $\ln(m_\ell/m)$ . At a given order, the logarithmic terms that do not vanish as  $m_\ell/m \rightarrow 0$  can often be computed from the knowledge of the lower order terms and of the  $\beta$  function through the renormalization group equations [24, 25, 26, 27].

These general properties already allow to draw several elementary conclusions. The electron being the lightest charged lepton, its anomalous magnetic moment is dominantly determined by the values of the coefficients  $A_n$ . The first contribution of other degrees of freedom comes from graphs involving, say, at least one muon loop, which occurs first at the two-loop level, and is of the order of  $(m_e/m_\mu)^2(\alpha/\pi)^2 \sim 10^{-10}$ . The hadronic effects, i.e. “quark and gluon loops”, characterized by a scale of  $\sim 1$  GeV, or effects of degrees of freedom beyond the standard model, which may appear at some high scale  $M$ , will be felt more strongly, by a considerable factor  $(m_\mu/m_e)^2 \sim 40\,000$ , in  $a_\mu$  than in  $a_e$ . Thus,  $a_e$  is well suited for testing the validity of QED at higher orders, whereas  $a_\mu$  is more appropriate for testing the weak sector of the standard model, one of the main motivations for the BNL experiment, and possibly for detecting new physics.

## Exercises for section 2

### Exercise 2.1

Show that the expression of the matrix element of the electromagnetic current given by Eqs. (2.4) and (2.5) indeed follows from the conditions stated. Show that the form factors  $F_i(k^2)$  in these equations are real if the current  $\mathcal{J}^\rho$  is hermitian. Work out the transformation properties of the different form factors under the operations of parity and time reversal. How many additional form factors are needed in order to describe the same matrix element if the assumption concerning the conservation of the current is dropped?

### Exercise 2.2

Show that the current  $\widehat{\mathcal{J}}^\rho$  defined by Eq. (2.8) is conserved.

---

<sup>7</sup>In the presence of the weak interactions, this statement has to be reconsidered. Indeed, the necessity for the cancellation of the  $SU(2) \times U(1)$  gauge anomalies [19, 20, 21] transforms the decoupling of, say, a single heavy fermion in a given generation, into a somewhat subtle issue [22, 23], the resulting lagrangian being no longer renormalizable.

### Exercise 2.3

Find the term one needs to add to  $\widehat{\mathcal{L}}_{\text{int}}$ , and thus to  $\widehat{\mathcal{J}}_\rho$ , such as to generate a constant but nonzero form factor  $\widehat{F}_4$  at tree level. Show that in the non relativistic limit it induces an interaction term of the form  $F_4(0)\boldsymbol{\sigma} \cdot (\boldsymbol{\nabla} \wedge \mathbf{B})$  in a non uniform magnetic field.

### Exercise 2.4

Show that the quantities  $\Lambda_i^\rho(p', p)$  defined in Eq. (2.15) indeed project on the corresponding form factors  $F_i(k^2)$  through Eq. (2.14). Derive Eqs. (2.16) and (2.17).

### Exercise 2.5

Work out the expression of the electromagnetic current in the standard model.

### Exercise 2.6

Give the most general decomposition of the matrix element in Eq. (2.5) in the case of a massive Majorana neutrino [hint: see Refs. [28, 29] for a rather complete treatment].

## 3 Brief overview of the experimental situation

### 3.1 Measurements of the magnetic moment of the electron

The first indication that the gyromagnetic factor of the electron is different from the value  $g_e = 2$  predicted by the Dirac theory came from the precision measurement of hyperfine splitting in hydrogen and deuterium [30]. The first measurement of the gyromagnetic factor of free electrons was performed in 1958 [31], with a precision of 3.6%. The situation began to improve with the introduction of experimental setups based on the Penning trap. Some of the successive values obtained over a period of forty years are shown in Table 1. Technical improvements, eventually allowing for the trapping of a single electron or positron, produced, in the course of time, an enormous increase in precision which, starting from a few percents, went through the ppm levels, before culminating at 4 ppb [parts per billion] in the last [32] of a series of experiments performed at the University of Washington in Seattle. The same experiment has also produced a measurement of the magnetic moment of the positron with the same accuracy, thus providing a test of *CPT* invariance at the level of  $10^{-12}$ ,

$$g_{e^-}/g_{e^+} = 1 + (0.5 \pm 2.1) \times 10^{-12}. \quad (3.1)$$

Assuming invariance under *CPT*, the weighted average of the electron and positron anomalous moments obtained in Ref. [32] gives [33, 34],

$$a_e^{\text{exp}} = 0.001\,159\,652\,188\,3(42). \quad (3.2)$$

An extensive survey of the literature and a detailed description of the various experimental aspects can be found in [35]. The earlier experiments are reviewed in [36].

### 3.2 Measurements of the magnetic moment of the muon

The anomalous magnetic moment of the muon has also been the subject of quite a few experiments. The very short lifetime of the muon,  $\tau_\mu = (2.19703 \pm 0.00004) \times 10^{-6} s$ , makes it necessary to proceed



Table 1: Some experimental determinations of the electron’s anomalous magnetic moment  $a_e$  with the corresponding relative precision.

0.001 19(5)	4.2%	[37]
0.001 165(11)	1%	[38]
0.001 116(40)	3.6%	[31]
0.001 160 9(2 4)	2 100 ppm	[39]
0.001 159 622(27)	23 ppm	[40]
0.001 159 660(300)	258 ppm	[41]
0.001 159 657 7(3 5)	3 ppm	[42]
0.001 159 652 41(20)	172 ppb	[43]
0.001 159 652 188 4(4 3)	4 ppb	[32]

in a completely different way in order to attain a high precision. The experiments conducted at CERN during the years 1968-1977 used a muon storage ring [for details, see [44] and references quoted therein]. The more recent experiments at the AGS in Brookhaven are based on the same concept. Pions are produced by sending a proton beam on a target. The pions subsequently decay into longitudinally polarized muons, which are captured inside a storage ring, where they follow a circular orbit in the presence of both a uniform magnetic field and a quadrupole electric field, the latter serving the purpose of stabilizing the orbits. The difference between the spin precession frequency and the orbit frequency is given by

$$\omega_s - \omega_c = -\frac{e}{m_\mu c} \left\{ a_\mu \mathbf{B} - \left[ a_\mu + \frac{1}{1 - \gamma^2} \right] \boldsymbol{\beta} \wedge \mathbf{E} \right\}, \quad (3.3)$$

where  $\boldsymbol{\beta}$  is the velocity of the muons, and  $\gamma$  is the corresponding Lorentz boost factor. Therefore, if  $\gamma$  is tuned to its “magic” value  $\gamma = \sqrt{1 + 1/a_\mu} = 29.3$ , the measurement of  $\omega_s - \omega_c$  and of the magnetic field  $\mathbf{B}$  allows to determine  $a_\mu$ . The spin direction of the muon is determined by detecting the electrons or positrons produced in the decay of the muons with an energy greater than some threshold energy  $E_t$ . The number of detected electrons  $N_e(t)$  decreases exponentially with time, the time constant being set by the muon’s lifetime  $\gamma\tau_\mu c$  in the laboratory frame, and is modulated by the frequency  $\omega_s - \omega_c$ ,

$$N_e(t) = N_0(E_t) e^{-t/\gamma\tau_\mu} \{1 + A(E_t) \cos[(\omega_s - \omega_c)t + \phi(E_t)]\}. \quad (3.4)$$

The observation of this time dependence thus provides the required measurement of  $\omega_s - \omega_c$ .

Several experimental results for the anomalous magnetic moment of the positively charged muon, obtained at the CERN PS or, more recently, at the BNL AGS, are recorded in Table 2. Notice that the relative errors are measured in ppm units, to be contrasted with the ppb level of accuracy achieved in the electron case. The four last values in Table 2 were obtained by the E821 experiment at BNL. They show a remarkable stability and a steady increase in precision, and now completely dominate the world average value. Further data, for negatively charged muons <sup>8</sup> are presently being analysed.

<sup>8</sup>The CERN experiment had also measured  $a_{\mu^-} = 0.001 165 937(12)$  with a 10 ppm accuracy, giving the average value  $a_\mu = 0.001 165 924(8.5)$ , with an accuracy of 7 ppm.

Table 2: Determinations of the anomalous magnetic moment of the positively charged muon from the storage ring experiments conducted at the CERN PS and at the BNL AGS.

0.001 166 16(31)	265 ppm	[45]
0.001 165 895(27)	23 ppm	[46]
0.001 165 911(11)	10 ppm	[47]
0.001 165 925(15)	13 ppm	[48]
0.001 165 919 1(5 9)	5 ppm	[49]
0.001 165 920 2(1 6)	1.3 ppm	[50]
0.001 165 920 3(8)	0.7 ppm	[51]

The aim of the Brookhaven Muon ( $g - 2$ ) Collaboration is to reach a precision of 0.35 ppm, but this will depend on whether the experiment will receive financial support to collect more data or not <sup>9</sup>.

For completeness, one should mention that Eq. (3.3) is only correct as long as the muon has no electric dipole moment. If this is not the case, the more general relation,

$$\boldsymbol{\omega}_s - \boldsymbol{\omega}_c = -\frac{e}{m_\mu c} \left\{ a_\mu \mathbf{B} - \left[ a_\mu + \frac{1}{1 - \gamma^2} \right] \boldsymbol{\beta} \wedge \mathbf{E} \right\} - \frac{2d_\mu}{\hbar} \{ \boldsymbol{\beta} \wedge \mathbf{B} + \mathbf{E} \}, \quad (3.5)$$

which holds for  $\boldsymbol{\beta} \cdot \mathbf{E} = \boldsymbol{\beta} \cdot \mathbf{B} = 0$ , has to be used. The additional term proportional to  $d_\mu$  induces an oscillation of the muon spin with respect to the plane of motion <sup>10</sup>. In the standard model, given the experimental precision and the intensities of the fields used in the experiment, it is quite legitimate to use the formula (3.3) instead of (3.5). However, in case a discrepancy arises between the experimental value of  $a_\mu$  and the standard model prediction, the difference could be induced by non standard contributions to either the anomalous magnetic moment  $a_\mu$  or the electric dipole moment  $d_\mu$ , see the discussion in [54].

### 3.3 Experimental bounds on the anomalous magnetic moment of the $\tau$ lepton

As already mentioned, the very short lifetime of the  $\tau$  precludes a measurement of its anomalous magnetic moment following any of the techniques described above. Indirect access to  $a_\tau$  is provided by the reaction  $e^+e^- \rightarrow \tau^+\tau^-\gamma$ . The results obtained by OPAL [56] and L3 [57] at LEP only lead to very loose bounds,

$$\begin{aligned} -0.052 < a_\tau < 0.058 \quad (95\%C.L.) \\ -0.068 < a_\tau < 0.065 \quad (95\%C.L.), \end{aligned} \quad (3.6)$$

<sup>9</sup>At the time of writing, the prospects in this respect are unfortunately rather dim.

<sup>10</sup>A measurement of the electric dipole moment of the muon was actually performed by the CERN experiment [47], with the result  $d_\mu = (3.7 \pm 3.4) \times 10^{-19}$  ecm. An even smaller value,  $d_\mu \lesssim 9.1 \times 10^{-25}$  ecm, can be inferred from the experimental value of the electric dipole moment of the electron [52, 53],  $d_e = 1.8(1.2)(1.0) \times 10^{-27}$ , ecm, and assuming a scaling law  $d_\mu \sim \frac{m_\mu}{m_e} d_e$ . Such a scaling law holds within the standard model, but not in models with flavour violating interactions, see for instance [54]. For a proposal to measure  $d_\mu$  at the level of  $\sim 10^{-24}$ , ecm, see [55].

respectively.

We shall now turn towards theory, in order to see how the standard model predictions compare with these experimental values. Only the cases of the electron and of the muon will be treated in some detail. The theoretical aspects as far as the anomalous magnetic moment of the  $\tau$  are concerned are discussed in [58] and in the references quoted therein.

## 4 The anomalous magnetic moment of the electron

We start with the anomalous magnetic moment of the lightest charged lepton, the electron. Since the electron mass  $m_e$  is much smaller than any other mass scale present in the standard model, the mass independent part of  $a_e^{\text{QED}}$  dominates its value. As mentioned before, non vanishing contributions appear at the level of the loop diagrams shown in Fig. 1.

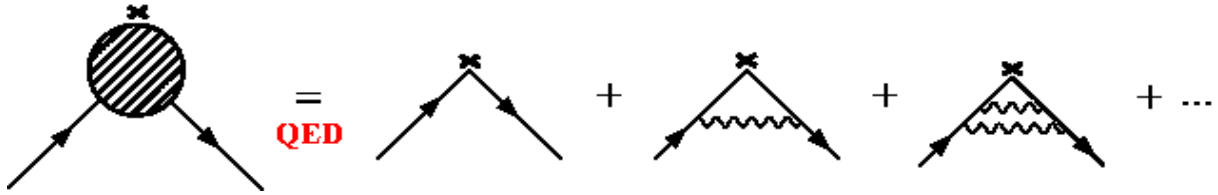


Figure 1: The perturbative expansion of  $\Gamma^\rho(p', p)$  in single flavour QED. The tree graph gives  $F_1 = 1$ ,  $F_2 = 0$ , whereas  $F_3(k^2)$  and  $F_4(k^2)$  vanish identically to all orders in pure QED. The one loop vertex correction graph gives the coefficient  $A_1$  in Eq. (2.21). The cross denotes the insertion of the external field.

### 4.1 The lowest order contribution

The one loop diagram gives

$$\begin{aligned} \Gamma^\rho(p', p)|_{1 \text{ loop}} &= (-ie)^2 \int \frac{d^4 q}{(2\pi)^4} \gamma^\mu \frac{i}{\not{p}' + \not{q} - m_e} \gamma^\rho \frac{i}{\not{p} + \not{q} - m_e} \gamma^\nu \\ &\quad \times \frac{(-i)}{q^2} \left[ \eta_{\mu\nu} - (1 - \xi) \frac{q_\mu q_\nu}{q^2} \right]. \end{aligned} \quad (4.1)$$

The photon propagator has been written in a Lorentz type gauge, corresponding to a covariant gauge fixing term  $-(\partial \cdot A)^2/2\xi$ . Let us for a moment concentrate on the  $\xi$  - dependence of this one loop expression. Recall that  $\Gamma^\rho(p', p)$  has eventually to be inserted between the spinors  $\bar{u}(p')$  and  $u(p)$ . Then, the gauge dependence of the integrand is given by

$$(1 - \xi) \bar{u}(p') \not{q} \frac{i}{\not{p}' + \not{q} - m_e} \gamma^\rho \frac{i}{\not{p} + \not{q} - m_e} \not{q} u(p) = (1 - \xi) \bar{u}(p') i \gamma_\rho i u(p),$$

and thus affects  $F_1(k^2)$ , but not  $F_2(k^2)$ . For evaluating the latter, one may therefore take, say,  $\xi = 1$  for convenience. The form factor  $F_2(k^2)$  is then obtained by using Eqs. (2.14) and (2.15) and, upon

evaluating the corresponding trace of Dirac matrices, one finds

$$F_2(k^2)|_{1 \text{ loop}} = ie^2 \frac{32m_e^2}{k^2(k^2 - 4m_e^2)^2} \int \frac{d^4q}{(2\pi)^4} \frac{1}{(p' + q)^2 - m_e^2} \frac{1}{(p + q)^2 - m_e^2} \frac{1}{q^2} \\ \times \left[ -3k^2(p \cdot q)^2 + 2k^2m_e^2(p \cdot q) + k^2m_e^2q^2 - m_e^2(k \cdot q)^2 \right]. \quad (4.2)$$

Then follow the usual steps of introducing two Feynman parameters, of performing a trivial change of variables and a symmetric integration over the loop momentum  $q$ , so that one arrives at

$$F_2(k^2)|_{1 \text{ loop}} = ie^2 \frac{64m_e^2}{(k^2 - 4m_e^2)^2} \int_0^1 dx \int_0^1 dy \int \frac{d^4q}{(2\pi)^4} \frac{1}{(q^2 - \mathcal{R}^2)^3} \\ \times \left[ 2x(1-x)m_e^4 - \frac{3}{4}x^2y^2(k^2)^2 + m_e^2k^2x \left( 3xy - y + \frac{1}{2}x \right) \right] \\ = \frac{e^2}{\pi^2} \frac{2m_e^2}{(k^2 - 4m_e^2)^2} \int_0^1 dx \int_0^1 dy \frac{1}{\mathcal{R}^2} \\ \times \left[ 2x(1-x)m_e^4 - \frac{3}{4}x^2y^2(k^2)^2 + m_e^2k^2x \left( 3xy - y + \frac{1}{2}x \right) \right], \quad (4.3)$$

with

$$\mathcal{R}^2 = x^2y(1-y)(2m_e^2 - k^2) + x^2y^2m_e^2 + x^2(1-y)^2m_e^2. \quad (4.4)$$

As expected, the limit  $k^2 \rightarrow 0$  can be taken without problem, and gives

$$a_e|_{1 \text{ loop}} \equiv F_2(0)|_{1 \text{ loop}} = \frac{1}{2} \frac{\alpha}{\pi}. \quad (4.5)$$

Let us stress that although the integral (4.1) diverges, we have obtained a finite result for  $F_2(k^2)$ , and hence for  $a_e$ , without introducing any regularization. This is of course expected, since a divergence in  $F_2(0)$  would require that a counterterm of the form given by the second term in  $\hat{\mathcal{L}}_{\text{int}}$ , see Eq. (2.8), be introduced. This would in turn spoil the renormalizability of the theory. In fact, as is well known, the divergence lies in  $F_1(0)$ , and goes into the renormalization of the charge of the electron.



Figure 2: The Feynman diagrams which contribute to the coefficient  $A_2$  in Eq. (2.21).

## 4.2 Higher order mass independent corrections

The previous calculation is rather straightforward and amounts to the result

$$A_1 = \frac{1}{2} \quad (4.6)$$

first obtained by Schwinger [59]. Schwinger's calculation was soon followed by a computation of  $A_2$  [60], which requires the evaluation of 7 graphs, representing five distinct topologies, and shown in Fig. 2. Historically, the result of Ref. [60] was important, because it provided the first explicit example of the realization of the renormalization program of QED at two loops. However, the value for  $A_2$  was not given correctly. The correct expression of the second order mass independent contribution was derived in [61, 62, 63] (see also [64, 65]) and reads <sup>11</sup>

$$\begin{aligned} A_2 &= \frac{197}{144} + \left(\frac{1}{2} - 3 \ln 2\right) \zeta(2) + \frac{3}{4} \zeta(3) \\ &= -0.328\,478\,965\dots \end{aligned} \quad (4.7)$$

with  $\zeta(p) = \sum_{n=1}^{\infty} 1/n^p$ ,  $\zeta(2) = \pi^2/6$ . The occurrence of transcendental numbers like  $\zeta(p)$  is a general feature of higher order calculations in perturbative quantum field theory. The pattern of these transcendentals in perturbation theory and the structure of the renormalization algorithm have also been put in relationship with other mathematical structures, like knot theory and braids [66], Hopf algebras [67] and non commutative geometry [68].

The analytic evaluation of the three loop mass independent contribution to the anomalous magnetic moment required quite some time, and is mainly due to the dedication of E. Remiddi and his coworkers during the period 1969-1996. There are now 72 diagrams to consider, involving many different topologies, see Fig. 3.

The calculation was completed [69] in 1996, with the analytical evaluation of a last class of diagrams, the non planar "triple cross" topologies. The result reads <sup>12</sup>

$$\begin{aligned} A_3 &= \frac{83}{72} \pi^2 \zeta(3) - \frac{215}{24} \zeta(5) + \frac{100}{3} \left[ \left( a_4 + \frac{1}{24} \ln^4 2 \right) - \frac{1}{24} \pi^2 \ln^2 2 \right] \\ &\quad - \frac{239}{2160} \pi^4 + \frac{139}{18} \zeta(3) - \frac{298}{9} \pi^2 \ln 2 + \frac{17101}{810} \pi^2 + \frac{28259}{5184} \\ &= 1.181\,241\,456\dots \end{aligned} \quad (4.8)$$

where <sup>13</sup>  $a_p = \sum_{n=1}^{\infty} \frac{1}{2^n n^p}$ . The numerical value extracted from the exact analytical expression given above can be improved to any desired order of precision.

<sup>11</sup>Actually, the experimental result of Ref. [38] disagreed with the value  $A_2 = -2.973$  obtained in [60], and prompted theoreticians to reconsider the calculation. The result obtained by the authors of Refs. [61, 62, 63] reconciled theory with experiment.

<sup>12</sup>The completion of this three-loop program can be followed through Refs. [70]-[75] and [69]. A description of the technical aspects related to this work and an account of its status up to 1990, with references to the corresponding literature, are given in Ref. [76].

<sup>13</sup>The first three values are known to be  $a_1 = \ln 2$ ,  $a_2 = \text{Li}_2(1/2) = (\zeta(2) - \ln^2 2)/2$ ,  $a_3 = \frac{7}{8} \zeta(3) - \frac{1}{2} \zeta(2) \ln 2 + \frac{1}{6} \ln^3 2$  [76].

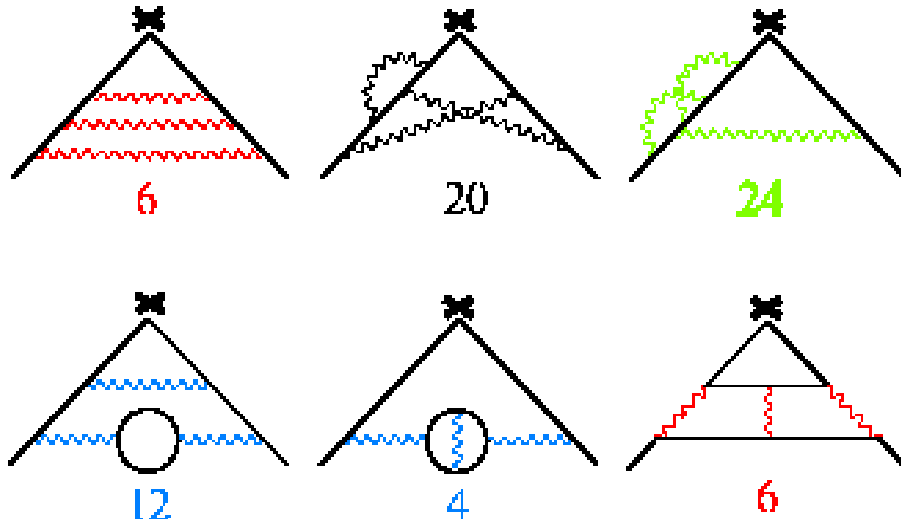


Figure 3: The 72 Feynman diagrams which make up the coefficient  $A_3$  in Eq. (2.21).

In parallel to these analytical calculations, numerical methods for the evaluation of the higher order contributions were also developed, in particular by Kinoshita and his collaborators (for details, see [77]). The numerical evaluation of the full set of three loop diagrams was achieved in several steps [78]-[84]. The value quoted in [84] is  $A_3 = 1.195(26)$ , where the error comes from the numerical procedure. In comparison, let us quote the value [85, 77]  $A_3 = 1.176\,11(42)$  obtained if only a subset of 21 three loop diagrams out of the original set of 72 is evaluated numerically, relying on the analytical results for the remaining 51 ones, and recall the value  $A_3 = 1.181\,241\,456\dots$  obtained from the full analytical evaluation. The error induced on  $a_e$  due to the numerical uncertainty in the second, more accurate, value is still  $\Delta(a_e) = 5.3 \times 10^{-12}$ , whereas the experimental error is only  $\Delta(a_e)|_{\text{exp}} = 4.3 \times 10^{-12}$ . This discussion shows that the analytical evaluations of higher loop contributions to the anomalous magnetic moment of the electron have a strong practical interest as far as the precision of the theoretical prediction is concerned, and which goes well beyond the mere intellectual satisfaction and technical skills involved in these calculations.<sup>14</sup>

At the four loop level, there are 891 diagrams to consider. Clearly, only a few of them have been evaluated analytically [86, 87]. The complete numerical evaluation of the whole set gave [85]  $A_4 = -1.434(138)$ . The development of computers allowed subsequent reanalyses to be more accurate, i.e.  $A_4 = -1.557(70)$  [88]. Until recently, the “latest of [these] constantly improving values” was [5]  $A_4 = -1.509\,8(384)$ . This calculation certainly represents a formidable task, and requires many elaborate technical tools. A descriptive account can be found in [77]. Let us mention, for completeness, that efforts to improve upon the evaluation of  $A_4$  are presently being pursued. Thus, a mistake has recently been found in an earlier computer code used for the evaluation of a subclass of four loop diagrams [89], whose contribution to  $A_4$  was  $A_{4;IV(d)} = -0.7503(60)$  [for the precise meaning of the notation, we refer the reader to Refs. [77] and [85]]. The corrected value reads instead [89]

<sup>14</sup>It is only fair to point out that the numerical values that are quoted here correspond to those given in the original references. It is to be expected that they would certainly improve if today’s numerical possibilities were used.

$A_{4;IV(d)} = -0.99072(10)$  [note also the impressive improvement in the precision]. By itself, this correction induces a 16% downward shift of the value of  $A_4$ , a far from trivial modification [see below]. At the present stage, the value of  $A_4$  reads

$$A_4 = -1.750\,2(384). \quad (4.9)$$

Needless to say, so far the five loop contribution  $A_5$  is unknown territory. On the other hand,  $(\alpha/\pi)^5 \sim 7 \times 10^{-14}$ , so that one may reasonably expect, in view of the present experimental situation, that its knowledge is not yet required.

### 4.3 Mass dependent QED corrections

We now turn to the QED loop contributions to the electron's anomalous magnetic moment involving the heavier leptons,  $\mu$  and  $\tau$ . The lowest order contribution of this type occurs at the two loop level,  $\mathcal{O}(\alpha^2)$ , and corresponds to a heavy lepton vacuum polarization insertion in the one loop vertex graph, cf. Fig. 4. Quite generally, the contribution to  $a_\ell$  arising from the insertion, into the one loop vertex correction, of a vacuum polarization graph due to a loop of lepton  $\ell'$ , reads [90, 91]<sup>15</sup>

$$B_2(\ell, \ell') = \frac{1}{3} \int_{4m_{\ell'}^2}^{\infty} ds \sqrt{1 - \frac{4m_{\ell'}^2}{s}} \frac{s + 2m_{\ell'}^2}{s^2} \int_0^1 dx \frac{x^2(1-x)}{x^2 + (1-x)\frac{s}{m_\ell^2}}. \quad (4.10)$$

If  $m_{\ell'} \gg m_\ell$ , the second integrand can be approximated by  $x^2 m_\ell^2/s$ , and one obtains [93]

$$B_2(\ell, \ell') = \frac{1}{45} \left( \frac{m_\ell}{m_{\ell'}} \right)^2 + \dots, \quad m_{\ell'} \gg m_\ell. \quad (4.11)$$

The complete expansion of  $B_2(\ell, \ell')$  for  $m_{\ell'} \gg m_\ell$  can be found in [71], from which we quote

$$\begin{aligned} B_2(\ell, \ell') &= \frac{1}{45} \left( \frac{m_\ell}{m_{\ell'}} \right)^2 + \frac{1}{70} \left( \frac{m_\ell}{m_{\ell'}} \right)^4 \ln \left( \frac{m_\ell}{m_{\ell'}} \right) + \frac{9}{19600} \left( \frac{m_\ell}{m_{\ell'}} \right)^4 \\ &+ \frac{4}{315} \left( \frac{m_\ell}{m_{\ell'}} \right)^6 \ln \left( \frac{m_\ell}{m_{\ell'}} \right) - \frac{131}{99225} \left( \frac{m_\ell}{m_{\ell'}} \right)^6 \\ &+ \mathcal{O} \left[ \left( \frac{m_\ell}{m_{\ell'}} \right)^8 \ln \left( \frac{m_\ell}{m_{\ell'}} \right) \right]. \end{aligned} \quad (4.12)$$

Numerically, this translates into [the values for the masses that were used read  $m_e = 0.510\,998\,902(21)$  MeV,  $m_\tau = 1\,776.99_{-0.26}^{+0.29}$  [34], and  $m_\mu/m_e = 206.768\,277(24)$  [94]]

$$\begin{aligned} B_2(e, \mu) &= 5.197 \times 10^{-7} \\ B_2(e, \tau) &= 1.838 \times 10^{-9}. \end{aligned} \quad (4.13)$$

<sup>15</sup>A trivial change of variable on  $s$  brings the expression (4.10) into the form given in [90, 91]. Furthermore, the analytical result obtained upon performing the double integration is available in [92].



Figure 4: The insertion of a muon vacuum polarization loop into the electron vertex correction (left) or of an electron vacuum polarization loop into the muon vertex correction (right).

For later use, it is interesting to briefly discuss the structure of Eq. (4.10). The quantity which appears under the integral is related to the cross section for the scattering of a  $\ell^+\ell^-$  pair into a pair  $(\ell')^+(\ell')^-$  at lowest order in QED,

$$\sigma_{\text{QED}}^{\ell^+\ell^-\rightarrow(\ell')^+(\ell')^-}(s) = \frac{4\pi\alpha^2}{3s^2} \sqrt{1 - \frac{4m_{\ell'}^2}{s}} (s + 2m_{\ell'}^2), \quad (4.14)$$

so that

$$B_2(\ell; \ell') = \frac{1}{3} \int_{4m_{\ell'}^2}^{\infty} \frac{ds}{s} K(s) R^{(\ell')}(s), \quad (4.15)$$

where<sup>16</sup>

$$K(s) = \int_0^1 dx \frac{x^2(1-x)}{x^2 + (1-x)\frac{s}{m_{\ell}^2}}, \quad (4.16)$$

and  $R^{(\ell')}(s)$  is the lowest order QED cross section  $\sigma_{\text{QED}}^{\ell^+\ell^-\rightarrow(\ell')^+(\ell')^-}(s)$  divided by the asymptotic form of the cross section of the reaction  $e^+e^- \rightarrow \mu^+\mu^-$  for  $s \gg m_{\mu}^2$ ,  $\sigma_{\infty}^{e^+e^-\rightarrow\mu^+\mu^-}(s) = \frac{4\pi\alpha^2}{3s}$ .

The three loop contributions with different lepton flavours in the loops are also known analytically [95, 96]. It is convenient to distinguish three classes of diagrams. The first group contains all the diagrams with one or two vacuum polarization insertion involving the same lepton,  $\mu$  or  $\tau$ , of the type shown in Fig. 5. The second group consists of the leptonic light-by-light scattering insertion diagrams, Fig. 6. Finally, since there are three flavours of massive leptons in the standard model, one has also the possibility of having graphs with two heavy lepton vacuum polarization insertions, one made of a muon loop, the other of a  $\tau$  loop. This gives

$$B_3(e, \ell) = B_3^{(\text{v.p.})}(e; \mu) + B_3^{(\text{v.p.})}(e; \tau) + B_3^{(\text{L}\times\text{L})}(e; \mu) + B_3^{(\text{L}\times\text{L})}(e; \tau) + B_3^{(\text{v.p.})}(e; \mu, \tau). \quad (4.17)$$

The analytical expression for  $B_3^{(\text{v.p.})}(e; \mu)$  can be found in Ref. [95], whereas [96] gives the corresponding result for  $B_3^{(\text{L}\times\text{L})}(e; \mu)$ . For practical purposes, it is both sufficient and more convenient to use their expansions in powers of  $m_e/m_{\mu}$ ,

$$B_3^{(\text{v.p.})}(e; \mu) = \left(\frac{m_e}{m_{\mu}}\right)^2 \left[ -\frac{23}{135} \ln\left(\frac{m_{\mu}}{m_e}\right) - \frac{2}{45}\pi^2 + \frac{10117}{24300} \right]$$

<sup>16</sup>Explicit expressions for  $K(s)$  are also available, but for many purposes, the integral representation given here turns out to be more convenient.



$$\begin{aligned}
& + \left(\frac{m_e}{m_\mu}\right)^4 \left[ \frac{19}{2520} \ln^2\left(\frac{m_\mu}{m_e}\right) - \frac{14233}{132300} \ln\left(\frac{m_\mu}{m_e}\right) + \frac{49}{768} \zeta(3) - \frac{11}{945} \pi^2 + \frac{2976691}{296352000} \right] \\
& + \mathcal{O}\left[\left(\frac{m_e}{m_\mu}\right)^6\right] \\
& = -0.000\,021\,768\dots
\end{aligned} \tag{4.18}$$

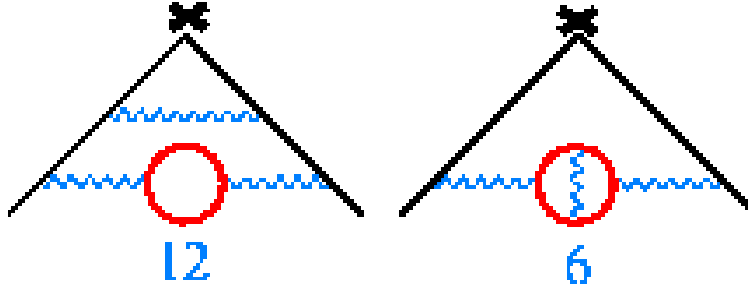


Figure 5: Three loop QED corrections with insertion of a heavy lepton vacuum polarization which make up the coefficient  $B_3^{(\text{v.p.})}(e; \mu)$ .

and

$$\begin{aligned}
B_3^{(\text{L}\times\text{L})}(e; \mu) & = \left(\frac{m_e}{m_\mu}\right)^2 \left[ \frac{3}{2} \zeta(3) - \frac{19}{16} \right] \\
& + \left(\frac{m_e}{m_\mu}\right)^4 \left[ -\frac{161}{810} \ln^2\left(\frac{m_\mu}{m_e}\right) - \frac{16189}{48600} \ln\left(\frac{m_\mu}{m_e}\right) + \frac{13}{18} \zeta(3) - \frac{161}{9720} \pi^2 - \frac{831931}{972000} \right] \\
& + \mathcal{O}\left[\left(\frac{m_e}{m_\mu}\right)^6\right] \\
& = 0.000\,014\,394\,5\dots
\end{aligned} \tag{4.19}$$

The expressions for  $B_3^{(\text{v.p.})}(e; \tau)$  and  $B_3^{(\text{L}\times\text{L})}(e; \tau)$  follow upon replacing the muon mass  $m_\mu$  by  $m_\tau$ . This again gives a suppression factor  $(m_\mu/m_\tau)^2$ , which makes these contributions negligible at the present level of precision. For the same reason,  $B_3^{(\text{v.p.})}(e; \mu, \tau)$  can also be discarded.

#### 4.4 Other contributions to $a_e$

In order to make the discussion of the standard model contributions to  $a_e$  complete, there remains to mention the hadronic and weak components,  $a_e^{\text{had}}$  and  $a_e^{\text{weak}}$ , respectively. Their features will be discussed in detail below, in the context of the anomalous magnetic moment of the muon. I therefore

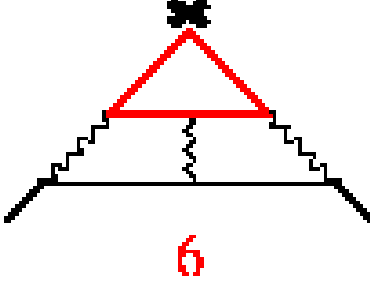


Figure 6: The three loop QED correction with the insertion of a heavy lepton light-by-light scattering subgraph, corresponding to the coefficient  $B_3^{(L \times L)}(e; \mu)$ .

only quote the numerical values <sup>17</sup>

$$a_e^{\text{had}} = 1.67(3) \times 10^{-12}, \quad (4.20)$$

and [97]

$$a_e^{\text{weak}} = 0.030 \times 10^{-12}. \quad (4.21)$$

#### 4.5 Comparison with experiment and determination of $\alpha$

Summing up the various contributions discussed so far gives the standard model prediction [4, 5, 8, 89]

$$a_e^{\text{SM}} = 0.5 \frac{\alpha}{\pi} - 0.328\,478\,444\,00 \left(\frac{\alpha}{\pi}\right)^2 + 1.181\,234\,017 \left(\frac{\alpha}{\pi}\right)^3 - 1.750\,2(38\,4) \left(\frac{\alpha}{\pi}\right)^4 + 1.70(3) \times 10^{-12}. \quad (4.22)$$

In order to obtain a number that can be compared to the experimental result, a sufficiently accurate determination of the fine structure constant  $\alpha$  is required. The best available measurement of the latter comes from the quantum Hall effect [33],

$$\alpha^{-1}(qH) = 137.036\,003\,00(2\,70) \quad (4.23)$$

and leads to

$$a_e^{\text{SM}}(qH) = 0.001\,159\,652\,146\,5(24\,0), \quad (4.24)$$

about six times less accurate than the experimental value of Eq. (3.2),  $a_e^{\text{exp}} = 0.001\,159\,652\,188\,3(4\,2)$ . On the other hand, if one excludes other contributions to  $a_e$  than those from the standard model considered so far, i.e. if one identifies  $a_e^{\text{SM}}$  with  $a_e^{\text{exp}}$ , then the value of  $a_e^{\text{exp}}$  as given in Eq. (3.2) provides the best determination of  $\alpha$  to date [89, 8],

$$\alpha^{-1}(a_e) = 137.035\,998\,75(5\,2), \quad (4.25)$$

at least to the extent that one may reasonably believe that all theoretical errors are under control. Now, as we have seen earlier, the value of  $A_4$  has recently been corrected [89]. The analysis presented

<sup>17</sup>I reproduce here the values given in [4, 5], except for the fact that I have taken into account the changes in the value of the hadronic light-by-light contribution to  $a_\mu$ , see below, for which I take  $a_\mu^{(L \times L)} = +8(4) \times 10^{-10}$ , and which translates into  $a_e^{(L \times L)} \sim a_\mu^{(L \times L)} (m_e/m_\mu)^2 = 0.02 \times 10^{-12}$ .

here incorporates the changes brought forward by the analysis of Ref. [89]. It lowers the prediction for  $a_e$  by  $\sim 7.0 \times 10^{-12}$  if one uses the value (4.23) of  $\alpha$ , or equivalently reduces the value of  $\alpha^{-1}(a_e)$  by one and a half standard deviation. It is very likely that the completion of the analysis begun in Ref. [89] will lead to a more accurate determination of  $A_4$ , and further changes in the numbers quoted here are to be expected.

## Exercises for section 4

### *Exercise 4.1*

Reproduce the steps that lead from Eq. (4.1) to Eq. (4.5).

## 5 The anomalous magnetic moment of the muon

In this section, the theoretical aspects concerning the anomalous magnetic moment of the muon are discussed. Since the muon is much heavier than the electron,  $a_\mu$  will be more sensitive to higher mass scales. In particular, it is a better probe for possible degrees of freedom beyond the standard model, like supersymmetry. The drawback, however, is that  $a_\mu$  will also be more sensitive to the non perturbative strong interaction dynamics at the  $\sim 1$  GeV scale.

### 5.1 QED contributions to $a_\mu$

As already mentioned before, the mass independent QED contributions to  $a_\mu$  are described by the same coefficients  $A_n$  as in the case of the electron. We therefore need only to discuss the coefficients  $B_n(\mu; \ell')$  associated with the mass dependent corrections.

For  $m_{\ell'} \ll m_\ell$ , Eq. (4.10) gives [90, 91, 92, 71]

$$B_2(\ell; \ell') = \frac{1}{3} \ln \left( \frac{m_\ell}{m_{\ell'}} \right) - \frac{25}{36} + \frac{\pi^2}{4} \frac{m_{\ell'}}{m_\ell} - 4 \left( \frac{m_{\ell'}}{m_\ell} \right)^2 \ln \left( \frac{m_\ell}{m_{\ell'}} \right) + 3 \left( \frac{m_{\ell'}}{m_\ell} \right)^2 + \mathcal{O} \left[ \left( \frac{m_{\ell'}}{m_\ell} \right)^3 \right]. \quad (5.1)$$

The complete expansion in powers of  $m_{\ell'}/m_\ell$  can again be found in [71]. In the case of  $B_2(\mu; \tau)$ , one may use the expression given in Eq. (4.12). Upon using the values  $m_e = 0.510998902(21)$  MeV,  $m_\mu = 105.658357(5)$  MeV,  $m_\tau = 1776.99^{+0.29}_{-0.26}$  MeV [34], and  $m_\mu/m_e = 206.768277(24)$  [94] the corresponding numbers read

$$B_2(\mu; e) = 1.094258300(38) \quad (5.2)$$

$$B_2(\mu; \tau) = 0.000078064(25). \quad (5.3)$$

Although these numbers follow from an analytical expression, there are uncertainties attached to them, induced by those on the corresponding values of the ratios of the lepton masses.

The three loop QED corrections decompose as

$$B_3(\mu, \ell) = B_3^{(\text{v.p.})}(\mu; e) + B_3^{(\text{v.p.})}(\mu; \tau) + B_3^{(\text{L} \times \text{L})}(\mu; e) + B_3^{(\text{L} \times \text{L})}(\mu; \tau) + B_3^{(\text{v.p.})}(\mu; e, \tau), \quad (5.4)$$

with [95, 96]

$$\begin{aligned}
B_3^{(\text{v.p.})}(\mu; e) &= \frac{2}{9} \ln^2 \left( \frac{m_\mu}{m_e} \right) + \left[ \zeta(3) - \frac{2}{3} \pi^2 \ln 2 + \frac{1}{9} \pi^2 + \frac{31}{27} \right] \ln \left( \frac{m_\mu}{m_e} \right) \\
&+ \frac{11}{216} \pi^4 - \frac{2}{9} \pi^2 \ln^2 2 - \frac{8}{3} a_4 - \frac{1}{9} \ln^4 2 - 3\zeta(3) + \frac{5}{3} \pi^2 \ln 2 - \frac{25}{18} \pi^2 + \frac{1075}{216} \\
&+ \frac{m_e}{m_\mu} \left[ -\frac{13}{18} \pi^3 - \frac{16}{9} \pi^2 \ln 2 + \frac{3199}{1080} \pi^2 \right] \\
&+ \left( \frac{m_e}{m_\mu} \right)^2 \left[ \frac{10}{3} \ln^2 \left( \frac{m_\mu}{m_e} \right) - \frac{11}{9} \ln \left( \frac{m_\mu}{m_e} \right) - \frac{14}{3} \pi^2 \ln 2 - 2\zeta(3) + \frac{49}{12} \pi^2 - \frac{131}{54} \right] \\
&+ \left( \frac{m_e}{m_\mu} \right)^3 \left[ \frac{4}{3} \pi^2 \ln \left( \frac{m_\mu}{m_e} \right) + \frac{35}{12} \pi^3 - \frac{16}{3} \pi^2 \ln 2 - \frac{5771}{1080} \pi^2 \right] \\
&+ \left( \frac{m_e}{m_\mu} \right)^4 \left[ -\frac{25}{9} \ln^3 \left( \frac{m_\mu}{m_e} \right) - \frac{1369}{180} \ln^2 \left( \frac{m_\mu}{m_e} \right) \right. \\
&+ \left. [-2\zeta(3) + 4\pi^2 \ln 2 - \frac{269}{144} \pi^2 - \frac{7496}{675}] \ln \left( \frac{m_\mu}{m_e} \right) \right. \\
&- \left. \frac{43}{108} \pi^4 + \frac{8}{9} \pi^2 \ln^2 2 + \frac{80}{3} a_4 + \frac{10}{9} \ln^4 2 - \frac{411}{32} \zeta(3) + \frac{89}{48} \pi^2 \ln 2 - \frac{1061}{864} \pi^2 - \frac{274511}{54000} \right] \\
&+ \mathcal{O} \left[ \left( \frac{m_e}{m_\mu} \right)^5 \right], \tag{5.5}
\end{aligned}$$

$$\begin{aligned}
B_3^{(\text{L}\times\text{L})}(\mu; e) &= \frac{2}{3} \pi^2 \ln \left( \frac{m_\mu}{m_e} \right) + \frac{59}{270} \pi^4 - 3\zeta(3) - \frac{10}{3} \pi^2 + \frac{2}{3} \\
&+ \frac{m_e}{m_\mu} \left[ \frac{4}{3} \pi^2 \ln \left( \frac{m_\mu}{m_e} \right) - \frac{196}{3} \pi^2 \ln 2 + \frac{424}{9} \pi^2 \right] \\
&+ \left( \frac{m_e}{m_\mu} \right)^2 \left[ -\frac{2}{3} \ln^3 \left( \frac{m_\mu}{m_e} \right) + \left( \frac{\pi^2}{9} - \frac{20}{3} \right) \ln^2 \left( \frac{m_\mu}{m_e} \right) - \left[ \frac{16}{135} \pi^4 + 4\zeta(3) - \frac{32}{9} \pi^2 + \frac{61}{3} \right] \ln \left( \frac{m_\mu}{m_e} \right) \right. \\
&+ \left. \frac{4}{3} \zeta(3) \pi^2 - \frac{61}{270} \pi^4 + 3\zeta(3) + \frac{25}{18} \pi^2 - \frac{283}{12} \right] \\
&+ \left( \frac{m_e}{m_\mu} \right)^3 \left[ \frac{10}{9} \pi^2 \ln \left( \frac{m_\mu}{m_e} \right) - \frac{11}{9} \pi^2 \right] \\
&+ \left( \frac{m_e}{m_\mu} \right)^4 \left[ \frac{7}{9} \ln^3 \left( \frac{m_\mu}{m_e} \right) + \frac{41}{18} \ln^2 \left( \frac{m_\mu}{m_e} \right) + \frac{13}{9} \pi^2 \ln \left( \frac{m_\mu}{m_e} \right) + \frac{517}{108} \ln \left( \frac{m_\mu}{m_e} \right) \right. \\
&+ \left. \frac{1}{2} \zeta(3) + \frac{191}{216} \pi^2 + \frac{13283}{2592} \right] + \mathcal{O} \left[ \left( \frac{m_e}{m_\mu} \right)^5 \right], \tag{5.6}
\end{aligned}$$

while  $B_3^{(\text{v.p.})}(\mu; \tau)$  and  $B_3^{(\text{L}\times\text{L})}(\mu; \tau)$  are derived from  $B_3^{(\text{v.p.})}(e; \mu)$  and from  $B_3^{(\text{L}\times\text{L})}(e; \mu)$ , respectively, by trivial substitutions of the masses. Furthermore, the graphs with mixed vacuum polarization insertions, one electron loop, and one  $\tau$  loop, are evaluated numerically using a dispersive integral [71, 95, 98].

Numerically, one obtains

$$\begin{aligned}
B_3^{(\text{v.p.})}(\mu; e) &= 1.920\,455\,1(2) \\
B_3^{(\text{L}\times\text{L})}(\mu; e) &= 20.947\,924\,7(7) \\
B_3^{(\text{v.p.})}(\mu; \tau) &= -0.001\,782\,3(5) \\
B_3^{(\text{L}\times\text{L})}(\mu; \tau) &= 0.002\,142\,9(7) \\
B_3^{(\text{v.p.})}(\mu; e, \tau) &= 0.000\,527\,7(2).
\end{aligned}
\tag{5.7}$$

Notice the large value of  $B_3^{(\text{L}\times\text{L})}(\mu; e)$ , due to the occurrence of terms involving factors like  $\ln(m_\mu/m_e) \sim 5$  and powers of  $\pi$ . Such a large contribution, first obtained numerically in Ref. [78], allowed to explain a discrepancy of  $1.7\sigma$  between the theoretical value and the experimental measurement of Ref. [45]. Finally, several pieces of  $B_3^{(\text{v.p.})}(\mu; e)$  had already been worked out earlier, in Refs. [24, 93, 99, 100, 101]

The contributions at fourth order in  $\alpha$  have been obtained numerically in Ref. [102]. They must be corrected for the change in  $A_4$  obtained in [89]. At the next order, no full calculation, even through numerical techniques, is available. Specific contributions, for instance those enhanced by powers of  $\ln(m_e/m_\mu)$  times powers of  $\pi$ , have been evaluated [103, 104, 105, 106].

Putting all these contributions together leads to the expression

$$a_\mu^{\text{QED}} = 0.5 \frac{\alpha}{\pi} + 0.765\,857\,399(45) \left(\frac{\alpha}{\pi}\right)^2 + 24.050\,509\,5(23) \left(\frac{\alpha}{\pi}\right)^3 + 125.08(41) \left(\frac{\alpha}{\pi}\right)^4 + 930(170) \left(\frac{\alpha}{\pi}\right)^5.
\tag{5.8}$$

Upon inserting the value of  $\alpha$  obtained from the anomalous magnetic moment of the electron in Eq. (4.25), one finds

$$a_\mu^{\text{QED}} = 11\,658\,470.35(28) \times 10^{-10}.
\tag{5.9}$$

## 5.2 Hadronic contributions to $a_\mu$

On the level of Feynman diagrams, hadronic contributions arise through loops of virtual quarks and gluons. These loops also involve the soft scales, and therefore cannot be computed reliably in perturbative QCD. We shall decompose the hadronic contributions into three subsets: hadronic vacuum polarization insertions at order  $\alpha^2$ , at order  $\alpha^3$ , and hadronic light-by-light scattering,

$$a_\mu^{\text{had}} = a_\mu^{(\text{h.v.p. } 1)} + a_\mu^{(\text{h.v.p. } 2)} + a_\mu^{(\text{h. L}\times\text{L})}
\tag{5.10}$$

### 5.2.1 Hadronic vacuum polarization

We first discuss  $a_\mu^{(\text{h.v.p. } 1)}$ , which arises at order  $\mathcal{O}(\alpha^2)$  from the insertion of a single hadronic vacuum polarization into the lowest order vertex correction graph, see Fig. 7. The importance of this contribution to  $a_\mu$  is known since long time [107, 108].

There is a very convenient dispersive representation of this diagram, similar to Eq. (4.10)

$$a_\mu^{(\text{h.v.p. } 1)} = 4\alpha^2 \int_{4M_\pi^2}^{\infty} \frac{ds}{s} K(s) \frac{1}{\pi} \text{Im}\Pi(s)$$

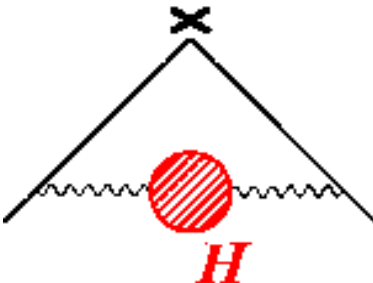


Figure 7: The insertion of the hadronic vacuum polarization into the one loop vertex correction, corresponding to  $a_\mu^{(\text{h.v.p. } 1)}$ .

$$= \frac{1}{3} \left( \frac{\alpha}{\pi} \right)^2 \int_{4M_\pi^2}^{\infty} \frac{ds}{s} K(s) R^{\text{had}}(s), \quad (5.11)$$

Here,  $\Pi(s)$  denotes the *hadronic* vacuum polarization function, defined as <sup>18</sup>

$$(q_\mu q_\nu - q^2 \eta_{\mu\nu}) \Pi(Q^2) = i \int d^4x e^{iq \cdot x} \langle \Omega | T \{ j_\mu(x) j_\nu(0) \} | \Omega \rangle, \quad (5.12)$$

with  $j_\rho$  the hadronic component of the electromagnetic current,  $Q^2 = -q^2 \geq 0$  for  $q_\mu$  spacelike, and  $|\Omega\rangle$  the QCD vacuum. The function  $K(s)$  was defined in Eq. (4.16), and  $R^{\text{had}}(s)$  stands now [see however below] for the cross section  $\sigma_0^{e^+e^- \rightarrow \text{had}}(s)$  of  $e^+e^- \rightarrow \text{hadrons}$ , *at lowest order in  $\alpha$* , divided by  $\sigma_\infty^{e^+e^- \rightarrow \mu^+\mu^-}(s) = \frac{4\pi\alpha^2}{3s}$ . A first principle computation of this strong interaction contribution is far beyond our present abilities to deal with the non perturbative aspects of confining gauge theories. This last relation is however very interesting because it expresses  $a_\mu^{(\text{h.v.p. } 1)}$  through a quantity that can be measured experimentally. In this respect, two important properties of the function  $K(s)$  deserve to be mentioned. First, it appears from the integral representation (4.16) that  $K(s)$  is positive definite. Since  $R^{\text{had}}$  is also positive, one deduces that  $a_\mu^{(\text{h.v.p. } 1)}$  itself is positive. Second, the function  $K(s)$  decreases as  $m_\mu^2/3s$  as  $s$  grows, so that it is indeed the low energy region which dominates the integral. Explicit evaluation of  $a_\mu^{(\text{h.v.p. } 1)}$  using available data actually reveals that more than 80% of its value comes from energies below 1.4 GeV. This observation is rather welcome, since the spectral density  $\text{Im}\Pi(s)$  can also be extracted from data on the hadronic decays of the  $\tau$  lepton in this energy region.

Finally, the values obtained in this way for  $a_\mu^{(\text{h.v.p. } 1)}$  have evolved in time, as shown in Table 3. This evolution is mainly driven by the availability of more data, and is still going on, as the last entries of Table 3 show. In order to match the precision reached by the latest experimental measurement of  $a_\mu$ ,  $a_\mu^{(\text{h.v.p. } 1)}$  needs to be known at  $\sim 1\%$ . Besides the very recent high quality  $e^+e^-$  data obtained by the BES Collaboration [109] in the region between 2 to 5 GeV, and by the CMD-2 collaboration [110] in the region dominated by the  $\rho$  resonance, the latest analyses sometimes also include or use, in the low-energy region, data obtained from hadronic decays of the  $\tau$  by ALEPH [111], and, more recently, by OPAL [112] and CLEO [113, 114]. We may notice from Table 3 that the precision obtained by using

<sup>18</sup>Actually,  $\Pi(s)$  defined this way has an ultraviolet divergence, produced by the QCD short distance singularity of the chronological product of the two currents. However, it only affects the real part of  $\Pi(s)$ . A renormalized, finite quantity is obtained by a single subtraction,  $\Pi(s) - \Pi(0)$ .

$e^+e^-$  data alone has become comparable to the one achieved upon including the  $\tau$  data. However, one of the latest analyses reveals a troubling discrepancy between the purely  $e^+e^-$  and the  $\tau$  based evaluations. Additional work is certainly needed in order to resolve these problems<sup>19</sup>. Further data are also expected in the future, from the KLOE experiment at the DAPHNE  $e^+e^-$  machine [124], or from the  $B$  factories BaBar [125] and Belle. For additional comparative discussions and details of the various analyses, we refer the reader to the literature quoted in Table 3. Averaging the results from the three most recent analysis with  $e^+e^-$  data only, from Refs. [121], [122], and [123], gives [8]

$$a_\mu^{(\text{h.v.p. } 1)}(e^+e^-) = 6838(75) \times 10^{-11}. \quad (5.13)$$

Table 3: Some of the recent evaluations of  $a_\mu^{(\text{h.v.p. } 1)} \times 10^{11}$  from  $e^+e^-$  and/or  $\tau$ -decay data. Note that the authors of Ref. [120] also use space like data for the pion form factor  $F_\pi(t)$ ; furthermore, they use a preliminary version of the CMD-2 data, that is now superseded by [110].

7024(153)	[115]	$e^+e^-$
7026(160)	[116]	$e^+e^-$
6950(150)	[117]	$e^+e^-$
7011(94)	[117]	$\tau, e^+e^-$ ,
6951(75)	[118]	$\tau, e^+e^-$ , QCD
6924(62)	[119]	$\tau, e^+e^-$ , QCD
7016(119)	[58]	$e^+e^-$ , QCD
7036(76)	[58]	$\tau, e^+e^-$ , QCD
7002(73)	[120]	$e^+e^-$ , incl. BES-II data, $F_\pi(t)$
6836(86)	[121]	$e^+e^-$ , incl. BES-II and CMD-2 data
6847(70)	[122]	$e^+e^-$ , incl. BES-II and CMD-2 data
7090(59)	[122]	$\tau, e^+e^-$ , incl. BES-II data
6831(62)	[123]	$e^+e^-$ , incl. BES-II and CMD-2 data

Let us briefly mention here that it is quite easy to estimate the order of magnitude of  $a_\mu^{(\text{h.v.p. } 1)}$ . For this purpose, it is convenient to introduce still another representation [2, 126], which relates  $a_\mu^{(\text{h.v.p. } 1)}$  to the hadronic Adler function  $\mathcal{A}(Q^2)$ , defined as<sup>20</sup>

$$\mathcal{A}(Q^2) = -Q^2 \frac{\partial \Pi(Q^2)}{\partial Q^2} = \int_0^\infty dt \frac{Q^2}{(t+Q^2)^2} \frac{1}{\pi} \text{Im}\Pi(t), \quad (5.14)$$

by

$$a_\mu^{(\text{h.v.p. } 1)} = 2\pi^2 \left(\frac{\alpha}{\pi}\right)^2 \int_0^1 \frac{dx}{x} (1-x)(2-x) \mathcal{A}\left(\frac{x^2}{1-x} m_\mu^2\right). \quad (5.15)$$

<sup>19</sup>For a possible explanation, see [8].

<sup>20</sup>Unlike  $\Pi(t)$  itself,  $\mathcal{A}(Q^2)$  is free from ultraviolet divergences.

A simple representation of the hadronic Adler function can be obtained if one assumes that  $\text{Im}\Pi(t)$  is given by a single, zero width, vector meson pole, and, above a certain threshold  $s_0$ , by the QCD perturbative continuum contribution,

$$\frac{1}{\pi} \text{Im}\Pi(t) = \frac{2}{3} f_V^2 M_V^2 \delta(t - M_V^2) + \frac{2}{3} \frac{N_C}{12\pi^2} [1 + \mathcal{O}(\alpha_s)] \theta(t - s_0) \quad (5.16)$$

The justification [127] for this type of minimal hadronic ansatz can be found within the framework of the large- $N_C$  limit [128, 129] of QCD, see Ref. [127] for a general discussion and a detailed study of this representation of the Adler function. The threshold  $s_0$  for the onset of the continuum expansion can be fixed from the property that in QCD there is no contribution in  $1/Q^2$  in the short distance expansion of  $\mathcal{A}(Q^2)$ , which requires [127]

$$2f_V^2 M_V^2 = \frac{N_C}{12\pi^2} s_0 \left( 1 + \frac{3}{8} \frac{\alpha_s(s_0)}{\pi} + \mathcal{O}(\alpha_s^2) \right). \quad (5.17)$$

This then gives  $a_\mu^{(\text{h.v.p. } 1)} \sim (570 \pm 170) \times 10^{-10}$ , which compares well with the more elaborate data based evaluations in Table 3, even though this simple estimate cannot claim to provide the required accuracy of about 1%.

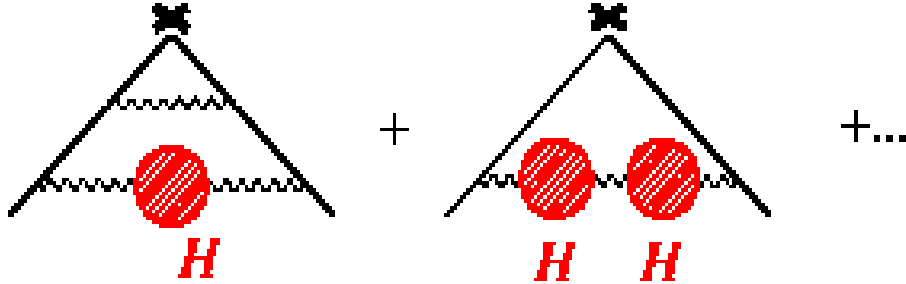


Figure 8: Higher order corrections containing the hadronic vacuum polarization contribution, corresponding to  $a_\mu^{(\text{h.v.p. } 2)}$ .

We now come to the  $\mathcal{O}(\alpha^3)$  corrections involving hadronic vacuum polarization subgraphs. Besides the contributions shown in Fig. 8, another one is obtained upon inserting a lepton loop in one of the two photon lines of the graph shown in Fig. 7. Taken all together, these can again be expressed in terms of  $R^{\text{had}}$  [130, 3, 98]

$$a_\mu^{(\text{h.v.p. } 2)} = \frac{1}{3} \left( \frac{\alpha}{\pi} \right)^3 \int_{4M_\pi^2}^{\infty} \frac{ds}{s} K^{(2)}(s) R^{\text{had}}(s). \quad (5.18)$$

The value obtained for this quantity is [98]

$$a_\mu^{(\text{h.v.p. } 2)} \times 10^{11} = -101 \pm 6. \quad (5.19)$$

The expression of  $K^{(2)}(s)$  is given in the references quoted above.



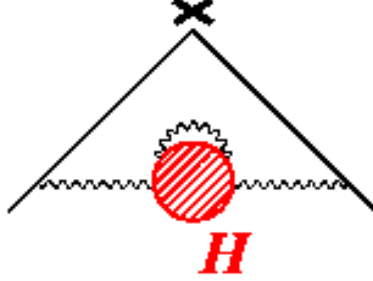


Figure 9: A higher order correction containing the hadronic vacuum polarization contribution, and which is included in  $a_\mu^{(\text{h.v.p. } 1)}$ .

There is actually another  $\mathcal{O}(\alpha^3)$  correction, namely the one obtained upon attaching a virtual photon line with both ends to the hadronic blob in Fig. 7, see Fig. 9. On the other hand,  $a_\mu^{(\text{h.v.p. } 1)}$  involves in principle data corrected for *all* electromagnetic effects. Whereas radiative corrections in the leptonic initial state and vacuum polarization effects in the photon propagator certainly can be accounted for, there is at present no way to handle in a model independent way electromagnetic corrections in the hadronic final state. These, on the other hand, contribute, together with final states containing an additional photon, to the  $\mathcal{O}(\alpha^3)$  contribution we have just been mentioning. It has become customary to include all these effects into  $a_\mu^{(\text{h.v.p. } 1)}$ , where it is then to be understood that  $R^{\text{had}}(s)$  in Eq. (5.11) actually stands for

$$R^{\text{had}}(s) = \frac{\sigma_0^{e^+e^- \rightarrow \text{had}}(s) + \sigma_2^{e^+e^- \rightarrow \text{had}}(s) + \sigma_0^{e^+e^- \rightarrow \text{had}+\gamma}(s)}{\sigma_\infty^{e^+e^- \rightarrow \mu^+\mu^-}(s)}, \quad (5.20)$$

where  $\sigma_0^{e^+e^- \rightarrow \text{had}}(s) + \sigma_2^{e^+e^- \rightarrow \text{had}}(s)$  denotes the cross section for  $e^+e^- \rightarrow \text{had}$  beyond leading order in the expansion in powers of the fine structure constant  $\alpha$ . The values given in Table 3 correspond to the definition (5.20). It also should be stressed that the next-to-leading cross section  $\sigma_2^{e^+e^- \rightarrow \text{had}}(s)$ , as well as the radiative cross section  $\sigma_0^{e^+e^- \rightarrow \text{had}+\gamma}(s)$ , are infrared divergent quantities, and only their sum is actually well defined.

### 5.2.2 Hadronic light-by-light scattering

We now discuss the so called hadronic light-by-light scattering graphs of Fig. 10.

The contribution to  $\Gamma_\rho(p', p)$  of relevance here is the matrix element, at lowest nonvanishing order in the fine structure constant  $\alpha$ , of the light quark electromagnetic current

$$j_\rho(x) = \frac{2}{3}(\bar{u}\gamma_\rho u)(x) - \frac{1}{3}(\bar{d}\gamma_\rho d)(x) - \frac{1}{3}(\bar{s}\gamma_\rho s)(x) \quad (5.21)$$

between  $\mu^-$  states,

$$\begin{aligned} (-ie)\bar{u}(p')\Gamma_\rho^{(\text{h. L}\times\text{L})}(p', p)u(p) &\equiv \langle \mu^-(p') | (ie)j_\rho(0) | \mu^-(p) \rangle \\ &= \int \frac{d^4q_1}{(2\pi)^4} \int \frac{d^4q_2}{(2\pi)^4} \frac{(-i)^3}{q_1^2 q_2^2 (q_1 + q_2 - k)^2} \end{aligned}$$

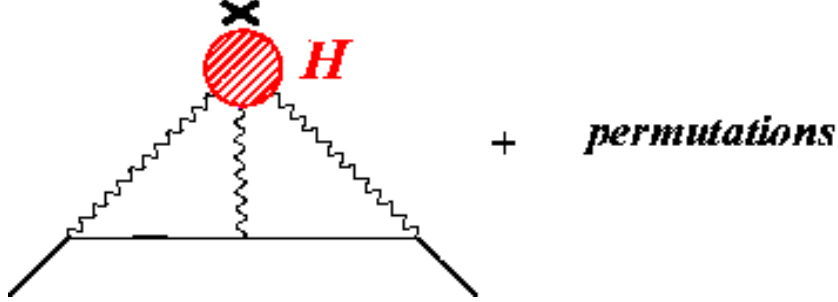


Figure 10: The hadronic light-by-light scattering graphs contributing to  $a_\mu^{(\text{h. L}\times\text{L})}$ .

$$\begin{aligned}
& \times \frac{i}{(p' - q_1)^2 - m^2} \frac{i}{(p' - q_1 - q_2)^2 - m^2} \\
& \times (-ie)^3 \bar{u}(p') \gamma^\mu (\not{p}' - \not{q}_1 + m) \gamma^\nu (\not{p}' - \not{q}_1 - \not{q}_2 + m) \gamma^\lambda u(p) \\
& \times (ie)^4 \Pi_{\mu\nu\lambda\rho}(q_1, q_2, k - q_1 - q_2), \tag{5.22}
\end{aligned}$$

with  $k_\mu = (p' - p)_\mu$  and

$$\begin{aligned}
\Pi_{\mu\nu\lambda\rho}(q_1, q_2, q_3) &= \int d^4x_1 \int d^4x_2 \int d^4x_3 e^{i(q_1 \cdot x_1 + q_2 \cdot x_2 + q_3 \cdot x_3)} \\
&\quad \times \langle \Omega | T \{ j_\mu(x_1) j_\nu(x_2) j_\lambda(x_3) j_\rho(0) \} | \Omega \rangle \tag{5.23}
\end{aligned}$$

the fourth-rank light quark hadronic vacuum-polarization tensor,  $|\Omega\rangle$  denoting the QCD vacuum. Since the flavour diagonal current  $j_\mu(x)$  is conserved, the tensor  $\Pi_{\mu\nu\lambda\rho}(q_1, q_2, q_3)$  satisfies the Ward identities

$$\{q_1^\mu; q_2^\nu; q_3^\lambda; (q_1 + q_2 + q_3)^\rho\} \Pi_{\mu\nu\lambda\rho}(q_1, q_2, q_3) = \{0; 0; 0; 0\}. \tag{5.24}$$

This entails that <sup>21</sup>

$$\bar{u}(p') \Gamma_\rho^{(\text{h. L}\times\text{L})}(p', p) u(p) = \bar{u}(p') \left[ \gamma_\rho F_1^{(\text{h. L}\times\text{L})}(k^2) + \frac{i}{2m} \sigma_{\rho\tau} k^\tau F_2^{(\text{h. L}\times\text{L})}(k^2) \right] u(p), \tag{5.25}$$

as well as  $\Gamma_\rho^{(\text{h. L}\times\text{L})}(p', p) = k^\tau \Gamma_{\rho\tau}^{(\text{h. L}\times\text{L})}(p', p)$  with

$$\begin{aligned}
\bar{u}(p') \Gamma_{\rho\sigma}^{(\text{h. L}\times\text{L})}(p', p) u(p) &= -ie^6 \int \frac{d^4q_1}{(2\pi)^4} \int \frac{d^4q_2}{(2\pi)^4} \frac{1}{q_1^2 q_2^2 (q_1 + q_2 - k)^2} \\
&\quad \times \frac{1}{(p' - q_1)^2 - m^2} \frac{1}{(p' - q_1 - q_2)^2 - m^2} \\
&\quad \times \bar{u}(p') \gamma^\mu (\not{p}' - \not{q}_1 + m) \gamma^\nu (\not{p}' - \not{q}_1 - \not{q}_2 + m) \gamma^\lambda u(p) \\
&\quad \times \frac{\partial}{\partial k^\rho} \Pi_{\mu\nu\lambda\sigma}(q_1, q_2, k - q_1 - q_2). \tag{5.26}
\end{aligned}$$

Following Ref. [78] and using the property  $k^\rho k^\sigma \bar{u}(p') \Gamma_{\rho\sigma}^{(\text{h. L}\times\text{L})}(p', p) u(p) = 0$ , one deduces that  $F_1^{(\text{h. L}\times\text{L})}(0) = 0$  and that the hadronic light-by-light contribution to the muon anomalous magnetic

<sup>21</sup>We use the following conventions for Dirac's  $\gamma$ -matrices:  $\{\gamma_\mu, \gamma_\nu\} = 2\eta_{\mu\nu}$ , with  $\eta_{\mu\nu}$  the flat Minkowski space metric of signature  $(+ - - -)$ ,  $\sigma_{\mu\nu} = (i/2)[\gamma_\mu, \gamma_\nu]$ ,  $\gamma_5 = i\gamma^0\gamma^1\gamma^2\gamma^3$ , whereas the totally antisymmetric tensor  $\varepsilon_{\mu\nu\rho\sigma}$  is chosen such that  $\varepsilon_{0123} = +1$ .

moment is equal to

$$a_\mu^{(\text{h. L}\times\text{L})} \equiv F_2^{(\text{h. L}\times\text{L})}(0) = \frac{1}{48m} \text{tr} \left\{ (\not{p} + m) [\gamma^\rho, \gamma^\sigma] (\not{p} + m) \Gamma_{\rho\sigma}^{(\text{h. L}\times\text{L})}(p, p) \right\}. \quad (5.27)$$

This is about all we can say about the QCD four-point function  $\Pi_{\mu\nu\lambda\rho}(q_1, q_2, q_3)$ . Unlike the hadronic vacuum polarization function, there is no experimental data which would allow for an evaluation of  $a_\mu^{(\text{h. L}\times\text{L})}$ . The existing estimates regarding this quantity therefore rely on specific models in order to account for the non perturbative QCD aspects. A few particular contributions can be identified, see Fig. 11. For instance, there is a contribution where the four photon lines are attached to a closed loop of charged mesons. The case of the charged pion loop with pointlike couplings is actually finite and contributes  $\sim 4 \times 10^{-10}$  to  $a_\mu$  [131]. If the coupling of charged pions to photons is modified by taking into account the effects of resonances like the  $\rho$ , this contribution is reduced by a factor varying between 3 [131, 132] and 10 [133], depending on the resonance model used. Another class of contributions consists of those involving resonance exchanges between photon pairs [131, 132, 133, 134]. Although here also the results depend on the models used, there is a constant feature that emerges from all the analyses that have been done: the contribution coming from the exchange of the pseudoscalars,  $\pi^0$ ,  $\eta$  and  $\eta'$  gives practically the final result. Other contributions [charged pion loops, vector, scalar, and axial resonances,...] are not only smaller, but also tend to cancel among themselves.

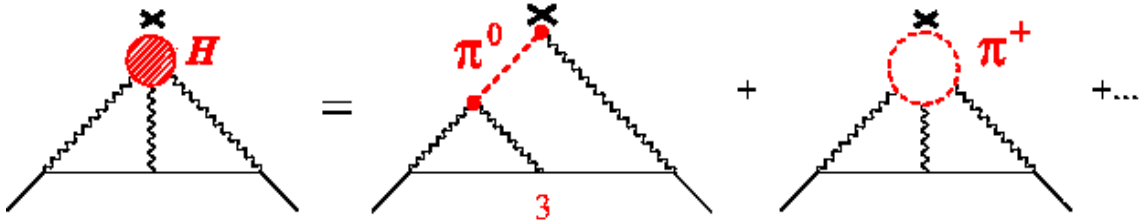


Figure 11: Some individual contributions to hadronic light-by-light scattering: the neutral pion exchange and the charged pion loop. There are other contributions, not shown here.

Some of the results obtained for  $a_\mu^{(\text{h. L}\times\text{L})}$  have been collected in Table 4. Leaving aside the first result [130, 3] shown there, which is affected by a bad numerical convergence [131], one notices that the sign of this contribution has changed twice. The first change resulted from a mistake in Ref. [131], that was corrected for in [133]. The minus sign that resulted was confirmed by an independent calculation, using the ENJL model, in Ref. [132]. A subsequent reanalysis [134] gave additional support to a negative result, while also getting better agreement with the value of Ref. [132].

Needless to say, these evaluations are based on heavy numerical work, which has the drawback of making the final results rather opaque to an intuitive understanding of the physics behind them. We [135] therefore decided to improve things on the analytical side, in order to achieve a better understanding of the relevant features that led to the previous results. Taking advantage of the observation that the pion exchange contribution  $a_\mu^{(\text{h. L}\times\text{L}; \pi^0)}$  was found to dominate the final values obtained for  $a_\mu^{(\text{h. L}\times\text{L})}$ , we concentrated our efforts on that part, that I shall now describe in greater detail. For a detailed account on how the other contributions to  $a_\mu^{(\text{h. L}\times\text{L})}$  arise, I refer the reader to the original works [131, 132, 133, 134].

Table 4: Various evaluations of  $a_\mu^{(\text{h. L}\times\text{L})} \times 10^{11}$  and of the pion pole contribution  $a_\mu^{(\text{h. L}\times\text{L};\pi^0)} \times 10^{11}$ .

-260(100)	constituent quark loop	[130, 3]
+60(4)	constituent quark loop	[131]
+49(5)	$\pi^\pm$ loop, $\pi^0$ and resonance exchanges, $a_\mu^{(\text{h. L}\times\text{L};\pi^0)} = +65(6)$	[131]
-92(32)	ENJL, $a_\mu^{(\text{h. L}\times\text{L};\pi^0+\eta+\eta')} = -85(13)$	[132]
-52(18)	$\pi^\pm$ loop, $\pi^0$ and resonance exchanges, and quark loop $a_\mu^{(\text{h. L}\times\text{L};\pi^0)} = -55.60(3)$	[133]
-79.2(15.4)	$\pi^\pm$ loop, $\pi^0$ pole and quark loop, $a_\mu^{(\text{h. L}\times\text{L};\pi^0)} = -55.60(3)$	[134]
+83(12)	$\pi^0$ , $\eta$ and $\eta'$ exchanges only	[135]
+89.6(15.4)	$\pi^\pm$ loop, $\pi^0$ pole and quark loop, $a_\mu^{(\text{h. L}\times\text{L};\pi^0)} = +55.60(3)$	[136]
+83(32)	ENJL, $a_\mu^{(\text{h. L}\times\text{L};\pi^0+\eta+\eta')} = +85(13)$	[137]

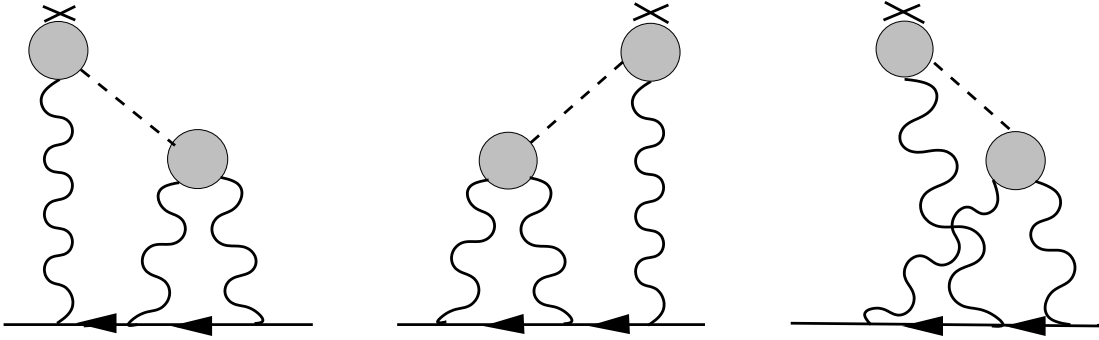


Figure 12: The pion-pole contributions to light-by-light scattering. The shaded blobs represent the form factor  $\mathcal{F}_{\pi^0\gamma^*\gamma^*}$ . The first and second graphs give rise to identical contributions, involving the function  $T_1(q_1, q_2; p)$  in Eq. (5.30), whereas the third graph gives the contribution involving  $T_2(q_1, q_2; p)$ .

The contributions to  $\Pi_{\mu\nu\lambda\rho}(q_1, q_2, q_3)$  due to single neutral pion exchanges, see Fig. 12, read

$$\begin{aligned}
 \Pi_{\mu\nu\lambda\rho}^{(\pi^0)}(q_1, q_2, q_3) &= i \frac{\mathcal{F}_{\pi^0\gamma^*\gamma^*}(q_1^2, q_2^2) \mathcal{F}_{\pi^0\gamma^*\gamma^*}(q_3^2, (q_1 + q_2 + q_3)^2)}{(q_1 + q_2)^2 - M_\pi^2} \varepsilon_{\mu\nu\alpha\beta} q_1^\alpha q_2^\beta \varepsilon_{\lambda\rho\sigma\tau} q_3^\sigma (q_1 + q_2)^\tau \\
 &+ i \frac{\mathcal{F}_{\pi^0\gamma^*\gamma^*}(q_1^2, (q_1 + q_2 + q_3)^2) \mathcal{F}_{\pi^0\gamma^*\gamma^*}(q_2^2, q_3^2)}{(q_2 + q_3)^2 - M_\pi^2} \varepsilon_{\mu\rho\alpha\beta} q_1^\alpha (q_2 + q_3)^\beta \varepsilon_{\nu\lambda\sigma\tau} q_2^\sigma q_3^\tau \\
 &+ i \frac{\mathcal{F}_{\pi^0\gamma^*\gamma^*}(q_1^2, q_3^2) \mathcal{F}_{\pi^0\gamma^*\gamma^*}(q_2^2, (q_1 + q_2 + q_3)^2)}{(q_1 + q_3)^2 - M_\pi^2} \varepsilon_{\mu\lambda\alpha\beta} q_1^\alpha q_3^\beta \varepsilon_{\nu\rho\sigma\tau} q_2^\sigma (q_1 + q_3)^\tau .
 \end{aligned} \tag{5.28}$$

The form factor  $\mathcal{F}_{\pi^0\gamma^*\gamma^*}(q_1^2, q_2^2)$ , which corresponds to the shaded blobs in Fig. 12, is defined as

$$i \int d^4x e^{iq \cdot x} \langle \Omega | T \{ j_\mu(x) j_\nu(0) \} | \pi^0(p) \rangle = \varepsilon_{\mu\nu\alpha\beta} q^\alpha p^\beta \mathcal{F}_{\pi^0\gamma^*\gamma^*}(q^2, (p-q)^2), \quad (5.29)$$

with  $\mathcal{F}_{\pi^0\gamma^*\gamma^*}(q_1^2, q_2^2) = \mathcal{F}_{\pi^0\gamma^*\gamma^*}(q_2^2, q_1^2)$ . Inserting the expression (5.28) into (5.26) and computing the corresponding Dirac traces in Eq. (5.27), we obtain

$$a_\mu^{(\text{h. L} \times \text{L}; \pi^0)} = e^6 \int \frac{d^4q_1}{(2\pi)^4} \int \frac{d^4q_2}{(2\pi)^4} \frac{1}{q_1^2 q_2^2 (q_1 + q_2)^2 [(p + q_1)^2 - m^2] [(p - q_2)^2 - m^2]} \\ \times \left[ \frac{\mathcal{F}_{\pi^0\gamma^*\gamma^*}(q_1^2, (q_1 + q_2)^2) \mathcal{F}_{\pi^0\gamma^*\gamma^*}(q_2^2, 0)}{q_2^2 - M_\pi^2} T_1(q_1, q_2; p) \right. \\ \left. + \frac{\mathcal{F}_{\pi^0\gamma^*\gamma^*}(q_1^2, q_2^2) \mathcal{F}_{\pi^0\gamma^*\gamma^*}((q_1 + q_2)^2, 0)}{(q_1 + q_2)^2 - M_\pi^2} T_2(q_1, q_2; p) \right], \quad (5.30)$$

where  $T_1(q_1, q_2; p)$  and  $T_2(q_1, q_2; p)$  denote two polynomials in the invariants  $p \cdot q_1$ ,  $p \cdot q_2$ ,  $q_1 \cdot q_2$ . Their expressions can be found in Ref. [135]. The former arises from the two first diagrams shown in Fig. 12, which give identical contributions, while the latter corresponds to the third diagram on this same figure. At this stage, it should also be pointed out that the expression (5.28) does not, strictly speaking, represent the contribution arising from the pion pole only. The latter would require that the numerators in (5.28) be evaluated at the values of the momenta that correspond to the pole indicated by the corresponding denominators. For instance, the numerator of the term proportional to  $T_1(q_1, q_2; p)$  in Eq. (5.30) should rather read  $\mathcal{F}_{\pi^0\gamma^*\gamma^*}(q_1^2, (q_1^2 + 2q_1 \cdot q_2 + M_\pi^2)) \mathcal{F}_{\pi^0\gamma^*\gamma^*}(M_\pi^2, 0)$  with  $q_2^2 = M_\pi^2$ . However, Eq. (5.30) corresponds to what previous authors have called the pion pole contribution, and which they had found to dominate the final result.

From here on, information on the form factor  $\mathcal{F}_{\pi^0\gamma^*\gamma^*}(q_1^2, q_2^2)$  is required in order to proceed. The simplest model for the form factor follows from the Wess-Zumino-Witten (WZW) term [138, 139] that describes the Adler-Bell-Jackiw anomaly [140, 141] in chiral perturbation theory. Since in this case the form factor is constant, one needs an ultraviolet cutoff, at least in the contribution to Eq. (5.30) involving  $T_1$ , the one involving  $T_2$  gives a finite result even for a constant form factor [131]. Therefore, this model cannot be used for a reliable estimate, but at best serves only illustrative purposes in the present context.<sup>22</sup> Previous calculations [131, 133, 134] have also used the usual vector meson dominance form factor [see also Ref. [143]]. The expressions for the form factor  $\mathcal{F}_{\pi^0\gamma^*\gamma^*}$  based on the ENJL model that have been used in Ref. [132] do not allow a straightforward analytical calculation of the loop integrals. However, compared with the results obtained in Refs. [131, 133, 134], the corresponding numerical estimates are rather close to the VMD case [within the error attributed to the model dependence]. Finally, representations of the form factor  $\mathcal{F}_{\pi^0\gamma^*\gamma^*}$ , based on the large- $N_C$  approximation to QCD and that takes into account constraints from chiral symmetry at low energies, and from the operator product expansion at short distances, have been discussed in Ref. [144]. They involve either one vector resonance [lowest meson dominance, LMD] or two vector resonances [LMD+V], see [144] for details. The four types of form factors just mentioned can be written in the

<sup>22</sup>In the context of an effective field theory approach, the pion pole with WZW vertices represents a chirally suppressed, but large- $N_C$  dominant contribution, whereas the charged pion loop is dominant in the chiral expansion, but suppressed in the large- $N_C$  limit [142].

form [ $F_\pi$  is the pion decay constant]

$$\mathcal{F}_{\pi^0\gamma^*\gamma^*}(q_1^2, q_2^2) = \frac{F_\pi}{3} \left[ f(q_1^2) - \sum_{M_{V_i}} \frac{1}{q_2^2 - M_{V_i}^2} g_{M_{V_i}}(q_1^2) \right]. \quad (5.31)$$

For the VMD and LMD form factors, the sum in Eq. (5.31) reduces to a single term, and the corresponding function is denoted  $g_{M_V}(q^2)$ . It depends on the mass  $M_V$  of the vector resonance, which will be identified with the mass of the  $\rho$  meson. For our present purposes, it is enough to consider only these two last cases, along with the constant WZW form factor. The corresponding functions  $f(q^2)$  and  $g_{M_V}(q^2)$  are displayed in Table 5.

Table 5: The functions  $f(q^2)$  and  $g_{M_V}(q^2)$  of Eq. (5.31) for the different form factors.  $N_C$  is the number of colours, taken equal to 3, and  $F_\pi = 92.4$  MeV is the pion decay constant. Furthermore,  $c_V = \frac{N_C}{4\pi^2} \frac{M_V^4}{F_\pi^2}$ .

	$f(q^2)$	$g_{M_V}(q^2)$
<i>WZW</i>	$-\frac{N_C}{4\pi^2 F_\pi^2}$	0
<i>VMD</i>	0	$\frac{N_C}{4\pi^2 F_\pi^2} \frac{M_V^4}{q^2 - M_V^2}$
<i>LMD</i>	$\frac{1}{q^2 - M_V^2}$	$-\frac{q^2 + M_V^2 - c_V}{q^2 - M_V^2}$

We may now come back to Eq. (5.30). With a representation of the form (5.31), the angular integrations can be performed, using for instance standard Gegenbauer polynomial techniques [hyperspherical approach], see Refs. [145, 146, 76]. This leads to a two dimensional integral representation:

$$a_\mu^{(\text{h. L} \times \text{L}; \pi^0)} = \left( \frac{\alpha}{\pi} \right)^3 \left[ a_\mu^{(\pi^0;1)} + a_\mu^{(\pi^0;2)} \right], \quad (5.32)$$

$$a_\mu^{(\pi^0;1)} = \int_0^\infty dQ_1 \int_0^\infty dQ_2 \left[ w_{f_1}(Q_1, Q_2) f^{(1)}(Q_1^2, Q_2^2) + w_{g_1}(M_V, Q_1, Q_2) g_{M_V}^{(1)}(Q_1^2, Q_2^2) \right], \quad (5.33)$$

$$a_\mu^{(\pi^0;2)} = \int_0^\infty dQ_1 \int_0^\infty dQ_2 \left[ \sum_{M=M_\pi, M_V} w_{g_2}(M, Q_1, Q_2) g_M^{(2)}(Q_1^2, Q_2^2) \right]. \quad (5.34)$$

The functions  $f^{(1)}(Q_1^2, Q_2^2)$ ,  $g_{M_V}^{(1)}(Q_1^2, Q_2^2)$ ,  $g_{M_\pi}^{(2)}(Q_1^2, Q_2^2)$  and  $g_{M_V}^{(2)}(Q_1^2, Q_2^2)$  are expressed in terms of the functions given in Table 5, see Ref. [135], where the universal [for the class of form factors that have a representation of the type shown in Eq. (5.31)] weight functions  $w_{f_1}$ ,  $w_{g_1}$ , and  $w_{g_2}$  in Eqs. (5.33) and (5.34) can also be found. The latter are shown in Fig. 13.

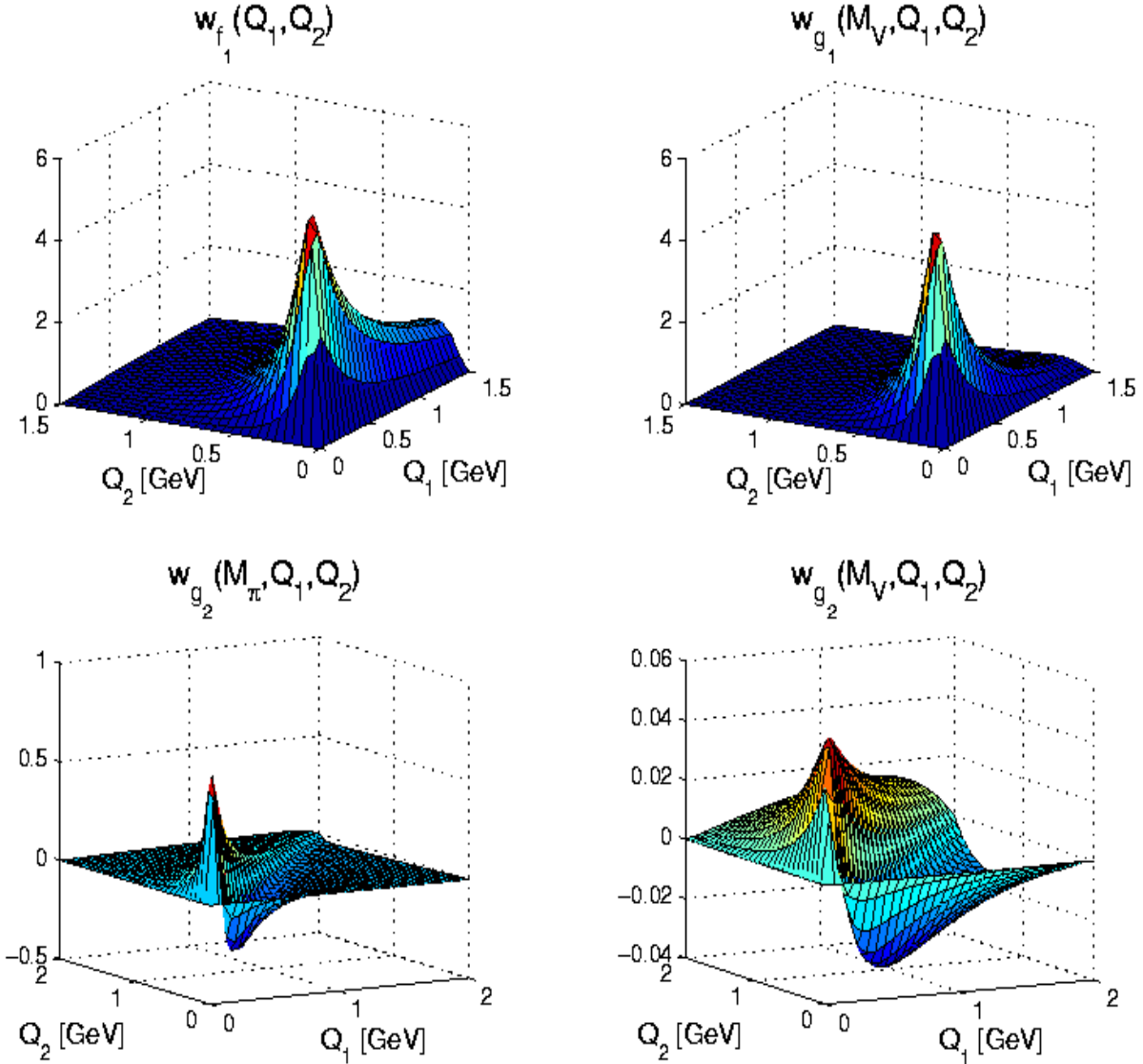


Figure 13: The weight functions appearing in Eqs. (5.33) and (5.34). Note the different ranges of  $Q_i$  in the subplots. The functions  $w_{f_1}$  and  $w_{g_1}$  are positive definite and peaked in the region  $Q_1 \sim Q_2 \sim 0.5$  GeV. Note, however, the tail in  $w_{f_1}$  in the  $Q_1$ -direction for  $Q_2 \sim 0.2$  GeV. The functions  $w_{g_2}(M_\pi, Q_1, Q_2)$  and  $w_{g_2}(M_V, Q_1, Q_2)$  take both signs, but their magnitudes remain small as compared to  $w_{f_1}(Q_1, Q_2)$  and  $w_{g_1}(M_V, Q_1, Q_2)$ . We have used  $M_V = M_\rho = 770$  MeV.

The functions  $w_{f_1}$  and  $w_{g_1}$  are positive and concentrated around momenta of the order of 0.5 GeV. This feature was already observed numerically in Ref. [132] by varying the upper bound of the integrals [an analogous analysis is contained in Ref. [133]]. Note, however, the tail in  $w_{f_1}$  in the  $Q_1$  direction for  $Q_2 \sim 0.2$  GeV. On the other hand, the function  $w_{g_2}$  has positive and negative contributions in that region, which will lead to a strong cancellation in the corresponding integrals, provided they are multiplied by a positive function composed of the form factors [see the numerical results below]. As

can be seen from the plots, and checked analytically, the weight functions vanish for small momenta. Therefore, the integrals are infrared finite. The behaviours of the weight functions for large values of  $Q_1$  and/or  $Q_2$  can also be worked out analytically. From these, one can deduce that in the case of the WZW form factor, the corresponding, divergent, integral for  $a_\mu^{(\pi^0;1)}$  behaves, as a function of the ultraviolet cut off  $\Lambda$ , as  $a_\mu^{(\pi^0;1)} \sim \mathcal{C} \ln^2 \Lambda$ , with [135]

$$\mathcal{C} = 3 \left( \frac{N_C}{12\pi} \right)^2 \left( \frac{m_\mu}{F_\pi} \right)^2 = 0.0248. \quad (5.35)$$

The log-squared behaviour follows from the general structure of the integral (5.33) for  $a_\mu^{(\pi^0;1)}$  in the case of a constant form factor, as pointed out in [6]. The expression (5.35) of the coefficient  $\mathcal{C}$  has been derived independently, in Ref. [147], through a renormalization group argument in the effective theory framework.

Table 6: Results for the terms  $a_\mu^{(\pi^0;1)}$ ,  $a_\mu^{(\pi^0;2)}$  and for the pion exchange contribution to the anomalous magnetic moment  $a_\mu^{(\text{h. L}\times\text{L};\pi^0)}$  according to Eq. (5.32) for the different form factors considered. In the WZW model, a cutoff of 1 GeV was used in the first contribution, whereas the second term is ultraviolet finite.

Form factor	$a_\mu^{(\pi^0;1)}$	$a_\mu^{(\pi^0;2)}$	$a_\mu^{(\text{h. L}\times\text{L};\pi^0)} \times 10^{10}$
WZW	0.095	0.0020	12.2
VMD	0.044	0.0013	5.6
LMD	0.057	0.0014	7.3

In the case of the other form factors, the integration over  $Q_1$  and  $Q_2$  is finite and can now be performed numerically.<sup>23</sup> Furthermore, since both the VMD and LMD model tend to the WZW constant form factor as  $M_V \rightarrow \infty$ , the results for  $a_\mu^{(\pi^0;1)}$  in these models should scale as  $\mathcal{C} \ln^2 M_V^2$  for a large resonance mass. This has been checked numerically, and the value of the coefficient  $\mathcal{C}$  obtained that way is in perfect agreement with the value given in Eq. (5.35). The results of the integration over  $Q_1$  and  $Q_2$  are displayed in Table 6. They definitely show a sign difference when compared to those obtained in Refs. [131, 133, 134, 143], although in absolute value the numbers agree perfectly. After the results of Table 6 were made public [135], previous authors checked their calculations and, after some time, discovered that they had made a sign mistake at some stage [136, 137]. The results presented in Table 6 and in Refs. [135, 147] have also received independent confirmations [149, 148].

The analysis of [135] leads to the following estimates

$$a_\mu^{(\text{h. L}\times\text{L};\pi^0)} = 5.8(1.0) \times 10^{-10}, \quad (5.36)$$

and

$$a_e^{(\text{h. L}\times\text{L};\pi^0)} = 5.1 \times 10^{-14}. \quad (5.37)$$

<sup>23</sup>In the case of the VMD form factor, an analytical result is now also available [148].



Taking into account the other contributions computed by previous authors, and adopting a conservative attitude towards the error to be ascribed to their model dependences, the total contribution to  $a_\mu$  coming from the hadronic light-by-light scattering diagrams amounts to

$$a_\mu^{(\text{h. L}\times\text{L})} = 8(4) \times 10^{-10}. \quad (5.38)$$

As a last remark, let me point out that the contribution depicted in Fig. 9 also involves the four point function  $\Pi_{\mu\nu\lambda\rho}(q_1, q_2, q_3)$ . It would be interesting to have an evaluation of this contribution to  $a_\mu^{(\text{h.v.p. 1})}$  based on the same models that were used to evaluate  $a_\mu^{\text{h. L}\times\text{L}}$ . The corresponding contribution arising from the neutral pion exchange has been evaluated in Ref. [148], but it is not obvious that it also dominates the complete result, since the kinematical configuration is different. This evaluation would also allow a direct comparison with the evaluations of Fig. 9 based on data.

### 5.3 Electroweak contributions to $a_\mu$

Electroweak corrections to  $a_\mu$  have been considered at the one and two loop levels. The one loop contributions, shown in Fig. 14, have been worked out some time ago, and read [150]-[154]

$$a_\mu^{\text{W}(1)} = \frac{G_F}{\sqrt{2}} \frac{m_\mu^2}{8\pi^2} \left[ \frac{5}{3} + \frac{1}{3} (1 - 4\sin^2 \theta_W)^2 + \mathcal{O}\left(\frac{m_\mu^2}{M_Z^2} \log \frac{M_Z^2}{m_\mu^2}\right) + \mathcal{O}\left(\frac{m_\mu^2}{M_H^2} \log \frac{M_H^2}{m_\mu^2}\right) \right], \quad (5.39)$$

where the weak mixing angle is defined by  $\sin^2 \theta_W = 1 - M_W^2/M_Z^2$ .

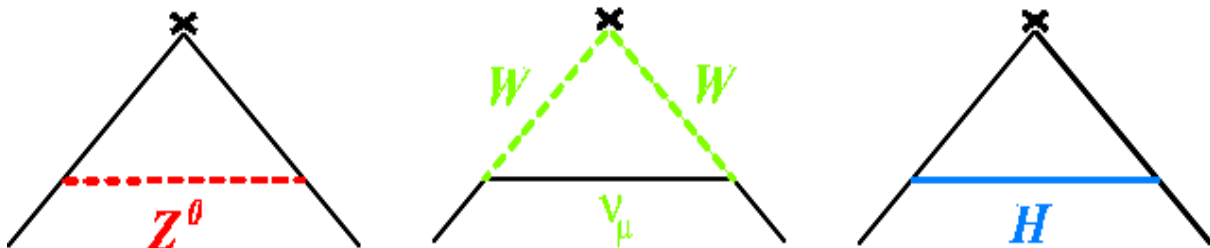


Figure 14: One loop weak interaction contributions to the anomalous magnetic moment.

Numerically, with  $G_F = 1.16639(1) \times 10^{-5} \text{ GeV}^{-2}$  and  $\sin^2 \theta_W = 0.224$ ,

$$a_\mu^{\text{W}(1)} = 194.8 \times 10^{-11}, \quad (5.40)$$

It is convenient to separate the two-loop electroweak contributions into two sets of Feynman graphs: those which contain closed fermion loops, which are denoted by  $a_\mu^{\text{EW}(2);f}$ , and the others,  $a_\mu^{\text{EW}(2);b}$ . In this notation, the electroweak contribution to the muon anomalous magnetic moment is

$$a_\mu^{\text{EW}} = a_\mu^{\text{W}(1)} + a_\mu^{\text{EW}(2);f} + a_\mu^{\text{EW}(2);b}. \quad (5.41)$$

I shall review the calculation of the two-loop contributions separately.

### 5.3.1 Two loop bosonic contributions

The leading logarithmic terms of the two-loop electroweak bosonic corrections have been extracted using asymptotic expansion techniques, see e.g. Ref. [155]. In the approximation where  $\sin^2 \theta_W \rightarrow 0$  and  $M_H \sim M_W$  these calculations simplify considerably and one obtains

$$a_\mu^{\text{EW}(2);b} = \frac{G_F}{\sqrt{2}} \frac{m_\mu^2}{8\pi^2} \frac{\alpha}{\pi} \times \left[ -\frac{65}{9} \ln \frac{M_W^2}{m_\mu^2} + \mathcal{O} \left( \sin^2 \theta_W \ln \frac{M_W^2}{m_\mu^2} \right) \right]. \quad (5.42)$$

In fact, these contributions have now been evaluated analytically, in a systematic expansion in powers of  $\sin^2 \theta_W$ , up to  $\mathcal{O}[(\sin^2 \theta_W)^3]$ , where  $\ln \frac{M_W^2}{m_\mu^2}$  terms,  $\ln \frac{M_H^2}{M_W^2}$  terms,  $\frac{M_W^2}{M_H^2} \ln \frac{M_H^2}{M_W^2}$  terms,  $\frac{M_W^2}{M_H^2}$  terms and constant terms are kept [97]. Using  $\sin^2 \theta_W = 0.224$  and  $M_H = 250 \text{ GeV}$ , the authors of Ref. [97] find

$$\begin{aligned} a_\mu^{\text{EW}(2);b} &= \frac{G_F}{\sqrt{2}} \frac{m_\mu^2}{8\pi^2} \frac{\alpha}{\pi} \times \left[ -5.96 \ln \frac{M_W^2}{m_\mu^2} + 0.19 \right] \\ &= \frac{G_F}{\sqrt{2}} \frac{m_\mu^2}{8\pi^2} \left( \frac{\alpha}{\pi} \right) \times [-78.9] = -21.1 \times 10^{-11}, \end{aligned} \quad (5.43)$$

showing, in retrospect, that the simple approximation in Eq. (5.42) is rather good.

### 5.3.2 Two loop fermionic contributions

The discussion of the two-loop electroweak fermionic corrections is more delicate. First, it contains a hadronic contribution. Next, because of the cancellation between lepton loops and quark loops in the electroweak  $U(1)$  anomaly, one cannot separate hadronic effects from leptonic effects any longer. In fact, as discussed in Refs. [156, 157], it is this cancellation which eliminates some of the large logarithms which, incorrectly were kept in Ref. [158]. It is therefore appropriate to separate the two-loop electroweak fermionic corrections into two classes: One is the class arising from Feynman diagrams containing a lepton or a quark loop, with the external photon, a virtual photon and a virtual  $Z^0$  attached to it, see Fig. 15.<sup>24</sup> The quark loop of course again represents non perturbative hadronic contributions which have to be evaluated using some model. This first class is denoted by  $a_\mu^{\text{EW}(2);f}(\ell; q)$ . It involves the QCD correlation function

$$W_{\mu\nu\rho}(q, k) = \int d^4x e^{iq \cdot x} \int d^4y e^{i(k-q) \cdot y} \langle \Omega | T \{ j_\mu(x) A_\nu^{(Z)}(y) j_\rho(0) \} | \Omega \rangle, \quad (5.44)$$

with  $k$  the incoming external photon four-momentum associated with the classical external magnetic field. As previously,  $j_\rho$  denotes the hadronic part of the electromagnetic current, and  $A_\rho^{(Z)}$  is the axial component of the current which couples the quarks to the  $Z^0$  gauge boson. The other class is defined by the rest of the diagrams, where quark loops and lepton loops can be treated separately, and is called  $a_\mu^{\text{EW}(2);f}(\text{residual})$ .

<sup>24</sup>If one works in a renormalizable gauge, the contributions where the  $Z^0$  is replaced by the neutral unphysical Higgs should also be included. The final result does not depend on the gauge fixing parameter  $\xi_Z$ , if one works in the class of 't Hooft gauges.

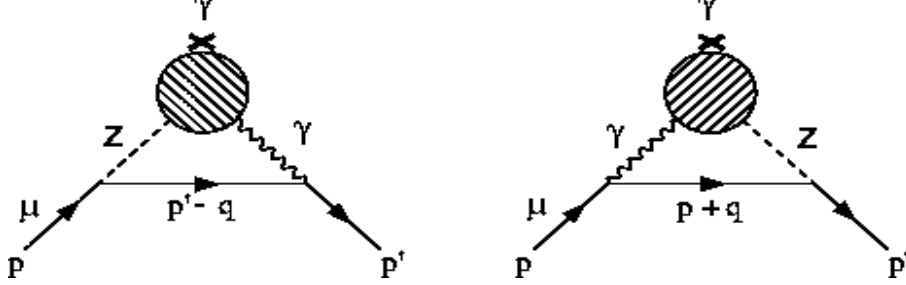


Figure 15: Graphs with hadronic contributions to  $a_\mu^{\text{EW}(2);f}(\ell, q)$  and involving the QCD three point function  $W_{\mu\nu\rho}(q, k)$ .

The contribution from  $a_\mu^{\text{EW}(2);f}(\text{residual})$  brings in factors of the ratio  $m_t^2/M_W^2$ . It has been evaluated, to a very good approximation, in Ref. [157], with the result

$$a_\mu^{\text{EW}(2);f}(\text{residual}) = \frac{G_F}{\sqrt{2}} \frac{m_\mu^2}{8\pi^2} \frac{\alpha}{\pi} \times \left[ \frac{1}{2 \sin^2 \theta_W} \left( -\frac{5}{8} \frac{m_t^2}{M_W^2} - \log \frac{m_t^2}{M_W^2} - \frac{7}{3} \right) + \Delta_{\text{Higgs}} \right], \quad (5.45)$$

where  $\Delta_{\text{Higgs}}$  denotes the contribution from diagrams with Higgs lines, which the authors of Ref. [157] estimate to be

$$\Delta_{\text{Higgs}} = -5.5 \pm 3.7, \quad (5.46)$$

and therefore,

$$a_\mu^{\text{EW}(2);f}(\text{residual}) = \frac{G_F}{\sqrt{2}} \frac{m_\mu^2}{8\pi^2} \frac{\alpha}{\pi} \times [-21(4)] = -5.6(1.4) \times 10^{-11}. \quad (5.47)$$

Let us finally discuss the contributions to  $a_\mu^{\text{EW}(2);f}(\ell; q)$ . Here, it is convenient to treat the contributions from the three generations separately. The contribution from the third generation can be calculated in a straightforward way, with the result [156, 157]

$$\begin{aligned} a_\mu^{\text{EW}(2);f}(\tau; t, b) &= \frac{G_F}{\sqrt{2}} \frac{m_\mu^2}{8\pi^2} \frac{\alpha}{\pi} \times \left[ -3 \ln \frac{M_Z^2}{m_\tau^2} - \ln \frac{M_Z^2}{m_b^2} - \frac{8}{3} \ln \frac{m_t^2}{M_Z^2} + \frac{8}{3} + \mathcal{O} \left( \frac{M_Z^2}{m_t^2} \ln \frac{m_t^2}{M_Z^2} \right) \right] \\ &= \frac{G_F}{\sqrt{2}} \frac{m_\mu^2}{8\pi^2} \frac{\alpha}{\pi} \times [-30.6] = -8.2 \times 10^{-11}. \end{aligned} \quad (5.48)$$

In fact the terms of  $\mathcal{O} \left( \frac{M_Z^2}{m_t^2} \ln \frac{m_t^2}{M_Z^2} \right)$  and  $\mathcal{O} \left( \frac{M_Z^2}{m_t^2} \right)$  have also been calculated in Ref. [157]. There are in principle QCD perturbative corrections to this estimate, which have not been calculated, but the result in Eq. (5.48) is good enough for the accuracy required at present. The contributions of the remaining charged standard model fermions involve the light quarks  $u$  and  $d$ , as well as the second generation  $s$  quark, for which non perturbative effects tied to the spontaneous breaking of chiral symmetry are important [156, 159]. The contributions from the first and second generation are thus most conveniently taken together, with the result

$$a_\mu^{\text{EW}(2);f}(e, \mu; u, d, s, c) = \frac{G_F}{\sqrt{2}} \frac{m_\mu^2}{8\pi^2} \frac{\alpha}{\pi} \times \left\{ -3 \ln \frac{M_Z^2}{m_\mu^2} - \frac{5}{2} \right.$$

$$\begin{aligned}
& -3 \ln \frac{M_Z^2}{m_\mu^2} + 4 \ln \frac{M_Z^2}{m_c^2} - \frac{11}{6} + \frac{8}{9} \pi^2 - 8 \\
& + \left[ \frac{4}{3} \ln \frac{M_Z^2}{m_\mu^2} + \frac{2}{3} + \mathcal{O} \left( \frac{m_\mu^2}{M_Z^2} \ln \frac{M_Z^2}{m_\mu^2} \right) \right] + 4.67(1.80) + 0.04(2) \Big\} \\
& = \frac{G_F}{\sqrt{2}} \frac{m_\mu^2}{8\pi^2} \frac{\alpha}{\pi} \times [-28.5(1.8)] = -7.6(5) \times 10^{-11}, \tag{5.49}
\end{aligned}$$

where the first line shows the result from the  $e$  loop and the second line the result from the  $\mu$  loop and the  $c$  quark, which is treated as a heavy quark. The term between brackets in the third line is the one induced by the anomalous term in the hadronic three point function  $W_{\mu\nu\rho}(q, k)$ . The other contributions have been estimated on the basis of an approximation to the large- $N_C$  limit of QCD, similar to the one discussed for the two-point function  $\Pi(Q^2)$  after Eq. (5.15), see Ref. [159] for details.

The result in Eq. (5.49) for the contribution from the first and second generations of quarks and leptons is conceptually rather different from the corresponding one proposed in Ref. [157],

$$\begin{aligned}
a_\mu^{\text{EW}(2);f}(e, \mu; u, d, s, c) &= \frac{G_F}{\sqrt{2}} \frac{m_\mu^2}{8\pi^2} \frac{\alpha}{\pi} \left[ -3 \ln \frac{M_Z^2}{m_\mu^2} + 4 \ln \frac{M_Z^2}{m_u^2} - \ln \frac{M_Z^2}{m_d^2} - \frac{5}{2} - 6 \right. \\
& \quad \left. - 3 \ln \frac{M_Z^2}{m_\mu^2} + 4 \ln \frac{M_Z^2}{m_c^2} - \ln \frac{M_Z^2}{m_s^2} - \frac{11}{6} + \frac{8}{9} \pi^2 - 6 \right] \\
&= \frac{G_F}{\sqrt{2}} \frac{m_\mu^2}{8\pi^2} \frac{\alpha}{\pi} \times [-31.9] = -8.5 \times 10^{-11}, \tag{5.50}
\end{aligned}$$

where the light quarks were, *arbitrarily*, treated the same way as heavy quarks, with  $m_u = m_d = 0.3 \text{ GeV}$ , and  $m_s = 0.5 \text{ GeV}$ . Numerically, the two expressions lead to similar results, though. A more recent analysis [160] provides a non perturbative treatment of the light quark sector, and gives

$$a_\mu^{\text{EW}(2);f}(e, \mu; u, d, s, c) = \frac{G_F}{\sqrt{2}} \frac{m_\mu^2}{8\pi^2} \frac{\alpha}{\pi} \times [-24.6] = -6.6 \times 10^{-11}. \tag{5.51}$$

The difference between the two results in Eqs. (5.49) and (5.51), which is numerically very small, is connected to interesting issues involving the anomalous  $\langle VVA \rangle$  three point function in QCD.<sup>25</sup>

The authors of Ref. [160] have also performed a detailed renormalization group analysis of the leading logarithm contributions at three loops<sup>26</sup>, and found them to be negligible. Taking into account other small effects that were previously neglected, their final value reads [160]

$$a_\mu^{\text{EW}} = 15.4(3) \times 10^{-10}, \tag{5.52}$$

which shows that the two-loop correction represents indeed a reduction of the one-loop result by an amount of 23%. The final error here includes uncertainties in the hadronic part, the variation of the Higgs mass in a range  $114 \text{ GeV} \leq M_H \leq 250 \text{ GeV}$ , the uncertainty on the mass of the top quark, and unknown three loop effects.

---

<sup>25</sup> Actually, the discussion centers around the transverse, i.e. *non anomalous* part of this QCD correlator, and is related to the existence of *non renormalization theorems* for it [161, 160, 162].

<sup>26</sup> See also [163].

## 5.4 Comparison with experiment

We may now put all the pieces together and obtain the value for  $a_\mu$  predicted by the standard model. We have seen that in the case of the hadronic vacuum polarization contributions, the latest evaluation [122] shows a discrepancy between the value obtained exclusively from  $e^+e^-$  data and the value that arises if  $\tau$  data are also included. This gives us the two possibilities

$$\begin{aligned} a_\mu^{\text{SM}}(e^+e^-) &= (11\,659\,167.5 \pm 7.5 \pm 4.0 \pm 0.4) \times 10^{-10} \\ a_\mu^{\text{SM}}(\tau) &= (11\,659\,192.7 \pm 5.9 \pm 4.0 \pm 0.4) \times 10^{-10}, \end{aligned} \tag{5.53}$$

where the first error comes from hadronic vacuum polarization, the second from hadronic light-by-light scattering, and the last from the QED and weak corrections. When compared to the present experimental average

$$a_\mu^{\text{exp}} = (11\,659\,203 \pm 8) \times 10^{-10} \tag{5.54}$$

there results a difference,

$$\begin{aligned} a_\mu^{\text{exp}} - a_\mu^{\text{SM}}(e^+e^-) &= 35.5(11.7) \times 10^{-10}, \\ a_\mu^{\text{exp}} - a_\mu^{\text{SM}}(\tau) &= 10.3(10.7) \times 10^{-10}, \end{aligned}$$

which represents 3.0 and 1.0 standard deviations, respectively.

Although experiment and theory have now both reached the same level of accuracy,  $\sim \pm 8 \times 10^{-10}$  or 0.7 ppm, the present discrepancy between the  $e^+e^-$  and  $\tau$  based evaluations makes the interpretation of the above results a delicate issue as far as evidence for new physics is concerned. Other evaluations of comparable accuracy [119, 120, 58] cover a similar range of variation in the difference between experiment and theory. Furthermore, the value obtained for  $a_\mu^{\text{SM}}(e^+e^-)$  relies strongly on the low-energy data obtained by the CMD-2 experiment, with none of the older data able to check them at the same level of precision. There seems to be an error in these data from the CMD-2 experiment [8], but this clearly needs to be confirmed. In this respect, the prospects for additional high statistics data in the future, either from KLOE or from BaBar, are most welcome. On the other hand, if the present discrepancy in the evaluations of the hadronic vacuum polarization finds a solution in the future, and if the experimental error is further reduced, by, say, a factor of two, then the theoretical uncertainty on the hadronic light-by-light scattering will constitute the next serious limitation on the theoretical side. It is certainly worthwhile to devote further efforts to a better understanding of this contribution, for instance by finding ways to feed more constraints with a direct link to QCD into the descriptions of the four-point function  $\Pi_{\mu\nu\rho\sigma}(q_1, q_2, q_3)$ .

## 6 Concluding remarks

With this review, I hope to have convinced the reader that the subject of the anomalous magnetic moments of the electron and of the muon is an exciting and fascinating topic. It provides a good example of mutual stimulation and strong interplay between experiment and theory.

The anomalous magnetic moment of the electron constitutes a very stringent test of QED and of the practical working of the framework of perturbatively renormalized quantum field theory at higher orders. It tests the validity of QED at very short distances, and provides at present the best determination of the fine structure constant.

The anomalous magnetic moment of the muon represents the best compromise between sensitivity to new degrees of freedom describing physics beyond the standard model and experimental feasibility. Important progress has been achieved on the experimental side during the last couple of years, with the results of the E821 collaboration at BNL. The experimental value of  $a_\mu$  is now known with an accuracy of 0.7ppm. Hopefully, the Brookhaven experiment will be given the opportunity to reach its initial goal of achieving a measurement at the 0.35 ppm level.

As can be inferred from the examples mentioned in this text, the subject constitutes, from a theoretical point of view, a difficult and error prone topic, due to the technical difficulties encountered in the higher loop calculations. The theoretical predictions have reached a precision comparable to the experimental one, but unfortunately there appears a discrepancy between the most recent evaluations of the hadronic vacuum polarization according to whether  $\tau$  data are considered or not. Hopefully, this situation will be clarified soon. Hadronic contributions, especially from vacuum polarization and from light-by-light scattering, are responsible for the bulk part of the final uncertainty in the theoretical value  $a_\mu^{\text{SM}}$ . Further efforts are needed in order to bring these aspects under better control.

**Acknowledgements:** I wish to thank A. Nyffeler, S. Peris, M. Perrottet, and E. de Rafael for stimulating and very pleasant collaborations. Most of the figures appearing in this text were kindly provided by M. Perrottet. A countless number of very informative and useful comments was provided by A. Nyffeler, M. Perrottet, and E. de Rafael. Finally, I wish to thank the organizers of the 41th edition of the Schlading school for their invitation to present these lectures and for providing, together with the students and the other lecturers, a very pleasant and fruitful atmosphere. This work is supported in part by the EC contract No. HPRN-CT-2002-00311 (EURIDICE).

## References

- [1] *Quantum Electrodynamics*, T. Kinoshita Ed., World Scientific Publishing Co. Pte. Ltd., 1990.
- [2] B. E. Lautrup, A. Peterman and E. de Rafael, Phys. Rept. **3**, 193 (1972).
- [3] J. Calmet, S. Narison, M. Perrottet and E. de Rafael, Rev. Mod. Phys. **49**, 21 (1977).
- [4] A. Czarnecki and W. J. Marciano, Nucl. Phys. B (Proc. Suppl.) **76**, 245 (1998).
- [5] V. W. Hughes and T. Kinoshita, Rev. Mod. Phys. **71**, S133 (1999).
- [6] K. Melnikov, Int. J. Mod. Phys. A **16**, 4591 (2001).
- [7] E. de Rafael, arXiv:hep-ph/0208251.
- [8] A. Nyffeler, to appear in the proceedings of the *38th Rencontres de Moriond on Electroweak Interactions and Unified Theories*, Les Arcs, 15-22 March 2003, and arXiv:hep-ph/0305135.

- [9] A. Czarnecki and W. J. Marciano, Phys. Rev. D **64**, 013014 (2001).
- [10] A list of recent papers on the subject can be found under the URL <http://www.slac.stanford.edu/spires/find/hep/www?c=PRLTA,86,2227>.
- [11] L. L. Foldy, Phys. Rev. **87**, 688 (1952); Rev. Mod. Phys. **30**, 471 (1958).
- [12] Ya. B. Zeldovich, Soviet Phys. JETP **6**, 1184 (1958).
- [13] Ya. B. Zeldovich and A. M. Perelomov, Soviet Phys. JETP **12**, 777 (1961).
- [14] R. E. Marshak, Riazuddin, and C. P. Ryan, *Theory of Weak Interactions in Particle Physics*, John Wiley and Sons Inc., 1969.
- [15] S. J. Brodsky and J. D. Sullivan, Phys. Rev. **156**, 1644 (1967).
- [16] R. Barbieri, J. A. Mignaco and E. Remiddi, Nuovo Cimento **11A**, 824 (1972).
- [17] H. Pietschmann, Zeit. f. Phys. **178**, 409 (1964).
- [18] T. Appelquist and J. Carazzone, Phys. Rev. D **11**, 2856 (1975).
- [19] C. Bouchiat, J. Iliopoulos and P. Meyer, Phys. Lett. **B38**, 519 (1972).
- [20] D. J. Gross and R. Jackiw, Phys. Rev. D **6**, 477 (1972).
- [21] C. P. Korthals Altes and M. Perrottet, Phys. Lett. B **39**, 546 (1972).
- [22] T. Sterling and M. J. Veltman, Nucl. Phys. **B 189**, 557 (1981).
- [23] E. d'Hoker and E. Farhi, Nucl. Phys. **B248**, 59, 77 (1984).
- [24] T. Kinoshita, Nuovo Cimento **51B**, 140 (1967).
- [25] B. E. Lautrup and E. de Rafael, Nucl. Phys. **B70**, 317 (1974).
- [26] E. de Rafael and J. L. Rosner, Ann. Phys. (N. Y.) **82**, 369 (1974).
- [27] T. Kinoshita and W. J. Marciano, *Theory of the Muon Anomalous Magnetic Moment*, in [1], p. 419.
- [28] B. Kayser, Phys. Rev. D **26**, 1662 (1982).
- [29] R. N. Mohapatra and P. B. Pal, *Massive Neutrinos in Physics and Astrophysics*, World Scientific Publishing Co. Pte. Ltd., 1991.
- [30] J. E. Nafe, E. B. Nelson and I. I. Rabi, Phys. Rev. **71**, 914 (1947).
- [31] H. G. Dehmelt, Phys. Rev. **109**, 381 (1958).
- [32] R. S. Van Dyck, P. B. Schwinberg and H. G. Dehmelt, Phys. Rev. Lett. **59**, 26 (1987).
- [33] P. J. Mohr and B. N. Taylor, Rev. Mod. Phys. **72**, 351 (2000).
- [34] K. Hagiwara *et al.* [Particle Data Group Collaboration], Phys. Rev. D **66**, 010001 (2002).

- [35] R. S. Van Dyck, *Anomalous Magnetic Moment of Single Electrons and Positrons: Experiment*, in [1], p. 322.
- [36] A. Rich and J. C. Wesley, *Rev. Mod. Phys.* **44**, 250 (1972).
- [37] P. Kusch and H. M. Fowley, *Phys. Rev.* **72**, 1256 (1947).
- [38] P. A. Franken and S. Liebes Jr., *Phys. Rev.* **104**, 1197 (1956).
- [39] A. A. Schuppe, R. W. Pidd, and H. R. Crane, *Phys. Rev.* **121**, 1 (1961).
- [40] D. T. Wilkinson and H. R. Crane, *Phys. Rev.* **130**, 852 (1963).
- [41] G. Grff, E. Klempt and G. Werth, *Z. Phys.* **222**, 201 (1968).
- [42] J. C. Wesley and A. Rich, *Phys. Rev. A* **4**, 1341 (1971).
- [43] R. S. Van Dyck, P. B. Schwinberg and H. G. Dehmelt, *Phys. Rev. Lett.* **38**, 310 (1977).
- [44] F. J. M. Farley and E. Picasso, *The Muon  $g - 2$  Experiments*, in [1], p. 479.
- [45] J. Bailey et al., *Phys. Lett.* **B28**, 287 (1968).
- [46] J. Bailey et al., *Phys. Lett.* **B55**, 420 (1975).
- [47] J. Bailey et al. [CERN-Mainz-Daresbury Collaboration], *Nucl. Phys.* **B 150**, 1 (1979).
- [48] R. M. Carey et al., *Phys. Rev. Lett.* **82**, 1632 (1999).
- [49] H. N. Brown et al. [Muon ( $g - 2$ ) Collaboration], *Phys. Rev. D* **62**, 091101(R) (2000).
- [50] H. N. Brown et al. [Muon ( $g - 2$ ) Collaboration], *Phys. Rev. Lett.* **86**, 2227 (2001).
- [51] G. W. Bennett et al. [Muon ( $g - 2$ ) Collaboration], *Phys. Rev. Lett.* **89**, 101804 (2002); Erratum-*ibid.* **89**, 129903 (2002).
- [52] E. D. Commins, S. B. Ross, D. DeMille and B. C. Regan, *Phys. Rev. A* **50**, 2960 (1994).
- [53] B. C. Regan, E. D. Commins, C. J. Schmidt and D. DeMille, *Phys. Rev. Lett.* **88**, 071805 (2002).
- [54] J. L. Feng, K. T. Matchev and Y. Shadmi, *Nucl. Phys.* **B 613**, 366 (2001); *Phys. Lett.* **B555**, 89 (2003).
- [55] Y. K. Semertzidis *et al.*, *Int. J. Mod. Phys. A* **16S1B**, 690 (2001).
- [56] K. Ackerstaff et al. [OPAL Collaboration], *Phys. Lett.* **B431**, 188 (1998).
- [57] M. Acciarri et al. [L3 Collaboration], *Phys. Lett.* **B434**, 169 (1998).
- [58] S. Narison, *Phys. Lett.* **B513**, 53 (2001); Erratum-*ibid.* **B526**, 414 (2002).
- [59] J. Schwinger, *Phys. Rev.* **73**, 413 (1948); **76**, 790 (1949).
- [60] R. Karplus and N. M. Kroll, *Phys. Rev.* **77**, 536 (1950).



- [61] A. Peterman, *Helv. Phys. Acta* **30**, 407 (1957).
- [62] C. M. Sommerfield, *Phys. Rev.* **107**, 328 (1957).
- [63] C. M. Sommerfield, *Ann. Phys. (N.Y.)* **5**, 26 (1958).
- [64] G. S. Adkins, *Phys. Rev. D* **39**, 3798 (1989).
- [65] J. Schwinger, *Particles, Sources and Fields, Volume III*, Addison-Wesley Publishing Company, Inc., 1989.
- [66] D. Kreimer, arXiv:hep-th/9412045; D. Kreimer, *J. Knot Theor. Ramifications* **6**, 479 (1997); D. J. Broadhurst, J. A. Gracey and D. Kreimer, *Z. Phys. C* **75**, 559 (1997); D. J. Broadhurst and D. Kreimer, *Phys. Lett.* **B393**, 403 (1997).
- [67] D. Kreimer, *Adv. Theor. Math. Phys.* **2**, 303 (1998).
- [68] A. Connes and D. Kreimer, *Commun. Math. Phys.* **199**, 203 (1998).
- [69] S. Laporta and E. Remiddi, *Phys. Lett.* **B379**, 283 (1996).
- [70] R. Barbieri and E. Remiddi, *Nucl. Phys.* **B 90**, 233 (1975).
- [71] M. A. Samuel and G. Li, *Phys. Rev. D* **44**, 3935 (1991); *ibid.* *D* **46**, 4782 (1992) and *D* **48**, 1879 (1993), errata.
- [72] S. Laporta and E. Remiddi, *Phys. Lett.* **B265**, 181 (1991).
- [73] S. Laporta, *Phys. Rev. D* **47**, 4793 (1993).
- [74] S. Laporta, *Phys. Lett.* **B343**, 421 (1995).
- [75] S. Laporta and E. Remiddi, *Phys. Lett.* **B356**, 390 (1995).
- [76] R. Z. Roskies, E. Remiddi and M. J. Levine, *Analytic evaluation of sixth-order contributions to the electron's g factor*, in [1], p. 162.
- [77] T. Kinoshita, *Theory of the anomalous magnetic moment of the electron – Numerical Approach*, in [1], p. 218.
- [78] J. Aldins, S. J. Brodsky, A. Dufner, and T. Kinoshita, *Phys. Rev. Lett.* **23**, 441 (1970); *Phys. Rev. D* **1**, 2378 (1970).
- [79] S. J. Brodsky and T. Kinoshita, *Phys. Rev. D* **3**, 356 (1971).
- [80] J. Calmet and M. Perrottet, *Phys. Rev. D* **3**, 3101 (1971).
- [81] J. Calmet and A. Peterman, *Phys. Lett.* **B47**, 369 (1973).
- [82] M. J. Levine and J. Wright, *Phys. Rev. Lett.* **26**, 1351 (1971); *Phys. Rev. D* **8**, 3171 (1973).
- [83] R. Carroll and Y. P. Yao, *Phys. Lett.* **B48**, 125 (1974).
- [84] P. Cvitanovic and T. Kinoshita, *Phys. Rev. D* **10**, 3978, 3991, 4007 (1974).

- [85] T. Kinoshita and W. B. Lindquist, Phys. Rev. D **27**, 867, 877, 886 (1983); D **39**, 2407 (1989); D **42**, 636 (1990).
- [86] M. Caffo, S. Turrini, and E. Remiddi, Phys. Rev. D **30**, 483 (1984).
- [87] E. Remiddi and S. P. Sorella, Lett. Nuovo Cim. **44**, 231 (1985).
- [88] T. Kinoshita, IEEE Trans. Instrum. Meas. **44**, 498 (1995).
- [89] T. Kinoshita and M. Nio, Phys. Rev. Lett. **90**, 021803 (2003).
- [90] H. Suura and E. Wichmann, Phys. Rev. **105**, 1930 (1957).
- [91] A. Peterman, Phys. Rev. **105**, 1931 (1957).
- [92] H. H. Elend, Phys. Lett. **20**, 682 (1966); Erratum-ibid. **21**, 720 (1966).
- [93] B. E. Lautrup and E. de Rafael, Phys. Rev. **174**, 1835 (1968).
- [94] W. Liu *et al.*, Phys. Rev. Lett. **82**, 711 (1999).
- [95] S. Laporta, Nuovo Cimento **106A**, 675 (1993).
- [96] S. Laporta and E. Remiddi, Phys. Lett. **B301**, 440 (1993).
- [97] A. Czarnecki, B. Krause and W. J. Marciano, Phys. Rev. Lett. **76**, 3267 (1996).
- [98] B. Krause, Phys. Lett. **B390**, 392 (1997).
- [99] B. E. Lautrup, Phys. Lett. **B32**, 627 (1970).
- [100] B. E. Lautrup and E. de Rafael, Nuovo Cim. **64A**, 322 (1970).
- [101] B. E. Lautrup, A. Peterman and E. de Rafael, Nuovo Cim. **1A**, 238 (1971).
- [102] T. Kinoshita, Phys. Rev. D **47**, 5013 (1993).
- [103] T. Kinoshita, B. Nizic, Y. Okamoto, Phys. Rev. D **41**, 593 (1990).
- [104] A. S. Yelkhovsky, Sov. J. Nucl. Phys. **49**, 656 (1989).
- [105] A. I. Milstein and A. S. Yelkhovsky, Phys. Lett. **B233**, 11 (1989).
- [106] S. G. Karshenboim, Phys. Atom. Nucl. **56**, 857 (1993).
- [107] C. Bouchiat and L. Michel, J. Phys. Radium **22**, 121 (1961).
- [108] L. Durand III, Phys. Rev. **128**, 441 (1962); Erratum-ibid. **129**, 2835 (1963).
- [109] J. Z. Bai et al. [BES Collaboration], Phys. Rev. Lett. **84**, 594 (2000); Phys. Rev. Lett. **88**, 101802 (2000).
- [110] R. R. Akhmetshin et al. [CMD-2 Collaboration], Phys. Lett. **B527**, 161 (2002).
- [111] R. Barate et al. [ALEPH Collaboration], Z. Phys. **C 2**, 123 (1997).

- [112] K. Ackerstaff et al. [OPAL Collaboration], *Eur. J. Phys. C* **7**, 571 (1999).
- [113] S. Anderson et al. [CLEO Collaboration], *Phys. Rev. D* **61**, 112002 (2000).
- [114] K. W. Edwards et al. [CLEO Collaboration], *Phys. Rev. D* **61**, 072003 (2000).
- [115] S. Eidelman and F. Jegerlehner, *Z. Phys. C* **67**, 585 (1995).
- [116] D. H. Brown and W. A. Worstell, *Phys. Rev. D* **54**, 3237 (1996).
- [117] R. Alemany, M. Davier and A. Höcker, *Eur. Phys. J. C* **2**, 123 (1998).
- [118] M. Davier and A. Höcker, *Phys. Lett.* **B419**, 419 (1998).
- [119] M. Davier and A. Höcker, *Phys. Lett.* **B435**, 427 (1998).
- [120] J. F. De Trocóniz and F. J. Ynduráin, *Phys. Rev. D* **65**, 093001 (2002).
- [121] F. Jegerlehner, *J. Phys. G* **29**, 101 (2003).
- [122] M. Davier, S. Eidelman, A. Höcker and Z. Zhang, *Eur. Phys. J. C* **27**, 497 (2003).
- [123] K. Hagiwara, A. D. Martin, D. Nomura and T. Teubner, *Phys. Lett. B* **557**, 69 (2003).
- [124] A. G. Denig *et al.* [the KLOE Collaboration], arXiv:hep-ex/0211024.
- [125] E. P. Solodov [BABAR collaboration], in *Proc. of the  $e^+e^-$  Physics at Intermediate Energies Conference* ed. Diego Bettoni, and arXiv:hep-ex/0107027.
- [126] M. Perrottet and E. de Rafael, unpublished.
- [127] S. Peris, M. Perrottet and E. de Rafael, *JHEP* **9805**, 011 (1998).
- [128] G. 't Hooft, *Nucl. Phys.* **B 72**, 461 (1974).
- [129] E. Witten, *Nucl. Phys.* **B 160**, 157 (1979).
- [130] J. Calmet, S. Narison, M. Perrottet and E. de Rafael, *Phys. Lett.* **B61**, 283 (1976).
- [131] T. Kinoshita, B. Nizic, Y. Okamoto, *Phys. Rev. D* **31**, 2108 (1985).
- [132] J. Bijnens, E. Pallante and J. Prades, *Nucl. Phys.* **B 474**, 379 (1996).
- [133] M. Hayakawa, T. Kinoshita and A. I. Sanda, *Phys. Rev. Lett.* **75**, 790 (1995); *Phys. Rev. D* **54**, 3137 (1996).
- [134] M. Hayakawa and T. Kinoshita, *Phys. Rev. D* **57**, 465 (1998).
- [135] M. Knecht and A. Nyffeler, *Phys. Rev. D* **65**, 073034 (2002).
- [136] M. Hayakawa and T. Kinoshita, arXiv:hep-ph/0112102, and the erratum to [134] published in *Phys. Rev. D* **66**, 019902(E) (2002).
- [137] J. Bijnens, E. Pallante and J. Prades, *Nucl. Phys.* **B 626**, 410 (2002).

- [138] J. Wess and B. Zumino, Phys. Lett. **37B**, 95 (1971).
- [139] E. Witten, Nucl. Phys. **B223**, 422 (1983).
- [140] S. L. Adler, Phys. Rev. **177**, 2426 (1969).
- [141] J. S. Bell and R. Jackiw, Nuovo Cimento A **60**, 47 (1969).
- [142] E. de Rafael, Phys. Lett. **B322**, 239 (1994).
- [143] J. Bijnens and F. Persson, arXiv:hep-ph/0106130.
- [144] M. Knecht and A. Nyffeler, Eur. Phys. J. C **21**, 659 (2001).
- [145] J. L. Rosner, Ann. Phys. (N.Y.) **44**, 11 (1967).
- [146] M. J. Levine and R. Roskies, Phys. Rev. D **9**, 421 (1974); M. J. Levine, E. Remiddi, and R. Roskies, *ibid.* **20**, 2068 (1979).
- [147] M. Knecht, A. Nyffeler, M. Perrottet and E. de Rafael, Phys. Rev. Lett. **88**, 071802 (2002).
- [148] I. Blokland, A. Czarnecki and K. Melnikov, Phys. Rev. Lett. **88**, 071803 (2002).
- [149] W. J. Bardeen and A. de Gouvea, private communication.
- [150] W.A. Bardeen, R. Gastmans and B.E. Lautrup, Nucl. Phys. **B46**, 315 (1972).
- [151] G. Altarelli, N. Cabbibo and L. Maiani, Phys. Lett. **40B**, 415 (1972).
- [152] R. Jackiw and S. Weinberg, Phys. Rev. D **5**, 2473 (1972).
- [153] I. Bars and M. Yoshimura, Phys. Rev. D **6**, 374 (1972).
- [154] M. Fujikawa, B.W. Lee and A.I. Sanda, Phys. Rev. D **6**, 2923 (1972).
- [155] V.A. Smirnov, Mod. Phys. Lett. A **10**, 1485 (1995).
- [156] S. Peris, M. Perrottet and E. de Rafael, Phys. Lett. **B355**, 523 (1995).
- [157] A. Czarnecki, B. Krause and W. Marciano, Phys. Rev. D **52**, R2619 (1995).
- [158] T.V. Kukhto, E.A. Kuraev, A. Schiller and Z.K. Silagadze, Nucl. Phys. **B 371**, 567 (1992).
- [159] M. Knecht, S. Peris, M. Perrottet and E. de Rafael, JHEP **0211**, 003 (2002).
- [160] A. Czarnecki, W. J. Marciano and A. Vainshtein, Phys. Rev. D **67**, 073006 (2003).
- [161] A. Vainshtein, arXiv:hep-ph/0212231.
- [162] M. Knecht, S. Peris, M. Perrottet and E. de Rafael, in preparation.
- [163] G. Degrossi and G.F. Giudice, Phys. Rev. **58D** (1998) 053007.